IEEE Access
Multidisciplinary | Rapid Review | Open Access Journal

Received June 25, 2017, accepted July 24, 2017, date of publication August 3, 2017, date of current version August 29, 2017.

Digital Object Identifier 10.1109/ACCESS.2017.2735865

INVITED PAPER

From Multi-Scale Decomposition to Non-Multi-Scale Decomposition Methods: A Comprehensive Survey of Image Fusion Techniques and Its Applications

AYUSH DOGRA, BHAWNA GOYAL, AND SUNIL AGRAWAL
Department of ECE, UIET, Panjab University, Chandigarh 160014, India
Corresponding author: Ayush Dogra (ayush123456789@gmail.com)

ABSTRACT Image fusion is a well-recognized and a conventional field of image processing. Image fusion provides an efficient way of enhancing and combining pixel-level data resulting in highly informative data for human perception as compared with individual input source data. In this paper, we have demonstrated a comprehensive survey of multi-scale and non-multi-scale decomposition-based image fusion methods in detail. The reference-based and non-reference-based image quality evaluation metrics are summarized together with recent trends in image fusion. Several image fusion applications in various fields have also been reported. It has been stated that though a lot of singular fusion techniques seemed to have given optimum results, the focus of researchers is shifting toward amalgamated or hybrid fusion techniques, which could harness the attributes of both multi-scale and non-multi-scale decomposition methods. Toward the end, the review is concluded with various open challenges for researchers. Thus, the descriptive study in this paper would form basis for stimulating and nurturing advanced research ideas in image fusion.

INDEX TERMS Image fusion, multi-scale decomposition, medical-imaging, sparse representation, fusion metrics, edge-information.

I. INTRODUCTION

The process of image fusion can be interpreted as to map the state of object, view, abnormality, modality and world into some easily perceptible lower dimensions [1], [2]. The images or data obtained from a single sensor does not suffice the accurate comprehension of the real state of the object in case of medical images or of the world in case of the remote sensing applications [3]. Hence there exists the wide spread and the ever growing interest in conglomerating the information from multiple sensors into a single image. Image fusion aims at developing a highly informative format of the data fetched from multisource or multisensory images into a single image. Multisensory image fusion has been extensively used in wide number of applications by academic researchers in the fields of mathematics, engineering sciences and physics. These groups of researchers are further classified into defence laboratories, corporate agencies and defence agencies and so on [4], [5].

Image fusion can be understood to be occurring at pixel level, feature level and decision level [6]. Pixel level image fusion refers to a type of fusion in which each new pixel of the fused image attains a different value based on combination of each of the pixels of the respective source images. It is also called image level fusion in some literature [2]. Pixel level image fusion can be viewed as the signal level fusion in two dimensions. Under feature level image fusion first the relevantly important features are extracted from each of the source images and then put together for some specific purposes e.g. fusion of edge maps [7], [8]. Decision level image fusion is a judgement based fusion and is also referred as symbol level fusion [7].

A fused image is an image in which each pixel is determined from a set of pixels in source images. Besides multisensory image fusion the various other classifications of image fusion based on the type of data sets are multi-focus, multi-view and multi-temporal [9]. However we will be concentrating mainly on the scope of multisensory image fusion in varied number of applications. The most advanced of sensors in current scenario includes optical cameras [10], x-ray imagers [11], DSA (Digital Subtraction Angiography)

machines [12]–[14], CT (Computed Tomography) scanners [15], MRI (Magnetic Resonance Imaging) scanners [16], infrared cameras and radar imagers [17], [18]. The set of images to be fused can be made available from different sensors of the same basic type or they can be coming from different type of sensors. To ensure a high quality image fusion, the images acquired from different sensors should be accurately aligned. This facilitates spatial registration which is essential for image fusion in the first place [19].

Multitasking, multi-monitoring, multi-analysis and parallel computing are the major attributes of image processing and computer vision. The working load of a human body operator increases manifold as multiple numbers of images require simultaneous monitoring and processing. However a human operator is not cent per cent reliable in assimilating the data presented by multiple images separately. Also the information obtained from multiple observers induces the margin of error in each one's interpretation. Besides subletting the human workload and error there arises a need of developing a practical image fusion system which has low cost and is time efficient. The images obtained from various sensors can be useful because they are complimentary and redundant. Multiple sensors providing redundant information can ensure reliability in case of sensor failure or error. Some sensors capture the various relative space domains of a particular image, fusing which provides the important complimentary information onto a single image. Hence image fusion is an extremely important field of application in remote sensing, defect inspection, concealed weapon detection and military surveillance. Another very important type of image fusion is multi-exposure image fusion. In this type of fusion images with varied luminance radiance are fused together to generate an image with higher dynamic range and with better visual quality. An over or under exposed area of an image carries far less information then the same area when well exposed. Therefore it is important to capture images with multiple exposures to capture details about an entire scene. Multi-exposure image fusion also finds its applications in high dynamic range (HDR) imaging techniques [20]. The advancement in the image fusion can be attributed to the evolution of various signal processing and analysis theory techniques which include multi-scale decompositions (MSD) [21], [22], multi-resolution analysis (MRA) [23], [24], intensity hue saturation (IHS) [25]–[27], principal component analysis (PCA) [28], dictionary learning [29], Brovey transform [30], hybrid methods [31], transform domain methods [32] and methods in other domains. In the beginning in 1997 a general introduction to image fusion in multisensory domain was given by Hall and Llinas [3]. In [1] Zhang and Blum gave a set of image fusion methods based on multi-scale decomposition. Then providing a complete edge over multi-scale decomposition methods, the advantageous multi-resolution properties of wavelet transform made them extremely popular in image processing [33]–[36]. To maintain the directional features of the images, the wavelet transform was further improvised in the form of discrete wavelet transform [37]–[39]. Besides these, several other state-of- the-art image fusion methods have been compared and analysed in [40] and [41]. The artificial neural networks (ANN) and image blocking algorithms have also been exploited in terms of image fusion [42]. The Shearlet and counterlet transform have been very efficiently used in non-sub-sampled domain in context of image fusion [43]–[47]. A comparison of image fusion methods in the field of remote sensing has been done in [48]. An excellent review on image fusion has been presented by Li *et al.* [49]. The current state-of-the-art in medical image fusion is summarized in [50]. Besides there are numerous algorithms devised for image fusion in literature. Some of them will be briefly reviewed in the context of this article. In this paper section 2 categorises the image fusion methods into multi-scale and non-multi-scale decomposition methods. The feature and the decision level image fusion are briefly discussed in section 3 and section 4 respectively. Section 5 discusses the various performance evaluation metrics for image fusion. Section 6 states the recent trends in the field of image fusion. Section 7 enlists the different applications of image fusion in the various fields. In section 8 an analytical contrast is drawn amongst the various image fusion techniques available in literature. Finally the article is concluded in section 9. The scope of this paper is mainly concentrated on the pixel level fusion methods. The prime search engines for this comprehensive survey were IEEE, Elsevier, Google scholar, PubMed. The major keywords used which helped fostering this article are image fusion, filters, sparse representation. The underlying idea was to follow the works of pioneer established scientists in field of image fusion. Some of them are R.S Blum, Shutao Li, Xudong Kang, Yu Liu, A. Toet, C.Pohl, Rui Shen, Peter Burt, V.P.S Naidu, B.K Shreyamsha, Subhasis Chaudhuri.

II. PIXEL LEVEL IMAGE FUSION

In the taxonomy of image fusion the pixel level image fusion is the most widely used type of image fusion in computer vision, remote sensing and medical imaging [51]–[54]. A plethora of image fusion techniques have been developed based on different algorithms. While it would be nearly impossible to discuss each of them we describe some of the most common approaches.

Majority of the image fusion methods comprises of three basic steps: mapping the image pixels in the transform domain, fusing the transformed coefficients and inverse transforming the fused coefficients to obtain the fused image [55]–[57].

First the acquired source images are accurately registered and then these images are fused. This can be illustrated in Fig. 1. Other popularly known categorization for image fusion methods is spatial domain methods; transform domain methods and dictionary learning methods [58]. Pixel level image fusion occurs at the lowest processing level which consists of merging of the measured physical parameters.

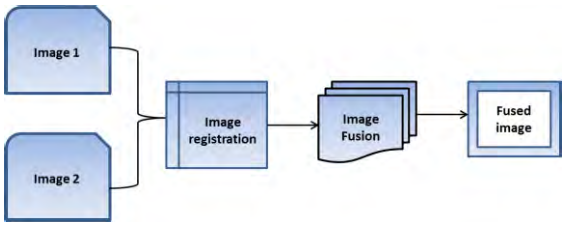

FIGURE 1. Block diagram for image fusion.

Based on image transform domain methodology pixel level image fusion can be divided into two major types: multi-scale decomposition methods and non-multi-scale decomposition methods [48]–[50]. Besides the transformation technique used for decomposition of source images, another very important role is played by the type of fusion strategy adopted. The commonly used image fusion strategies are weighted averaging [59], min-max rule [60]–[63], component substitution [64]–[66], machine learning [67], [68] region based consistency verification [69], cross-scale fusion [6], coefficient and window based strategies based on activity level measurement [70].

A. MULTI-SCALE DECOMPOSITION METHODS

Multi-scale decomposition has been acknowledged as a revolutionary tool which has proven to be extremely useful for image fusion. The most primitively employed multi-scale decomposition (MSD) methods were pyramidal transforms, discrete wavelet transform, and discrete wavelet frames. When an image is mapped into the respective pyramids the set of coefficients assume a pyramidal structure. A pyramidal structure can be imagined as a stack of image arrays at different scales representing the image as a whole. The most popular pyramidal representations are Laplacian pyramid transform (LPT) [71], [72], gradient pyramids [73], morphological pyramids [74], [75], steerable pyramids [76] and contrast pyramids [77]. The standard procedure for multi-scale image decomposition and reconstruction is described using Laplacian pyramids as follows [2].

Each level or pyramid of LPT is obtained by recursive decomposition of the source image into its lower levels. A band or a stage of the Laplacian pyramid is the difference of the two low pass images obtained using the Gaussian pyramids. This can be given as:

$$\vec{a}_k = \vec{J}_k - H\vec{J}_{k+1}$$

Where $H\vec{J}_{k+1}$ is an up-sampled, smoothed version of $\vec{J}_{k+1}$, so as to have same dimensions as $\vec{J}_k$ and $\vec{J}_0, \vec{J}_1, \vec{J}_2 \ldots\ldots\ldots \vec{J}_N$ represent the recursive stages of Gaussian pyramids.

$$H\vec{J}_{k+1} = \underbrace{\begin{bmatrix} .. & & & \\ & -g & & \\ & & -g & \\ & & & .... \end{bmatrix}}_{convolution} \underbrace{\begin{bmatrix} 1 & 0 & 0 & 0 \\ 0 & 0 & 0 & 0 \\ 0 & 1 & 0 & 0 \\ 0 & 0 & 0 & 0 \\ \ldots & \ldots & \ldots & \ldots \end{bmatrix}}_{up-sampling} \vec{J}_{k+1}$$

So the multi-scale decomposition using Laplacian pyramids can be summarized in four stages: Low pass filtering, sub-sampling, interpolation, and differencing. These steps of decomposition can be followed in inverse order to obtain the reconstructed image [2]. The generalised schematic for one stage of Laplacian pyramidal decomposition is illustrated in Fig. 2 below.

Once the multi-scale decompositions of the source images are obtained, these decompositions are fused together using any kind of fusion strategy to generate a multi-scale fused representation of the source images. The adopted fusion strategy depends on the choice of activity level measurement of coefficients, the correlation amongst the adjacent pixels, coefficient verification methods and coefficient combining methods. The fused image can be obtained by taking the inverse transform of the multi-scale representations. So an efficient fusion algorithm largely depends selection of the decomposition methods and the chosen fusion strategy for the combining the decomposed coefficients. Many researchers have attempted to find the perfect combination for the same. A brief review of various fusion strategies is listed below.

1) ACTIVITY LEVEL MEASUREMENT

Activity level gives the measure of the quality of a specific part of each of the source image. Activity level can be measured in the following ways: window based measures, coefficient based measures and region based measures. The window based activity (WBA) level measurement commonly employs a small squared window which is placed on the image with the coefficient under consideration at the centre. The common examples under this category include weighted average method [78] and rank filter method. The coefficient activity based measures quantifies each coefficient separately. The region based activity level measurement is similar to WBA except for region based methods have odd shapes. The various categorisation of activity level measurement methods can be understood from the following Fig. 3.

2) COEFFICIENT GROUPING METHOD

While we construct the fusion representation of MSD coefficients of two source images one can simply set each of the MSD coefficient of the source image onto the other. These coefficients can be related to the same pixel position in their low pass filtered image. The coefficient grouping is further divided into No Grouping (NG), Single Scale Grouping (SSG) and multi-scale grouping scheme [6], [80].

3) COEFFICIENT COMBINING METHOD

Coefficient combining method is one of the other alternatives to obtain composite multi-scale decomposition representations for the fused images. One method is Choose Max (CM) scheme which can be regarded as selecting the coefficient with higher activity and disregarding the one. Other example of coefficient combining methods is weighted averaging in which at each coefficient position x of the fused

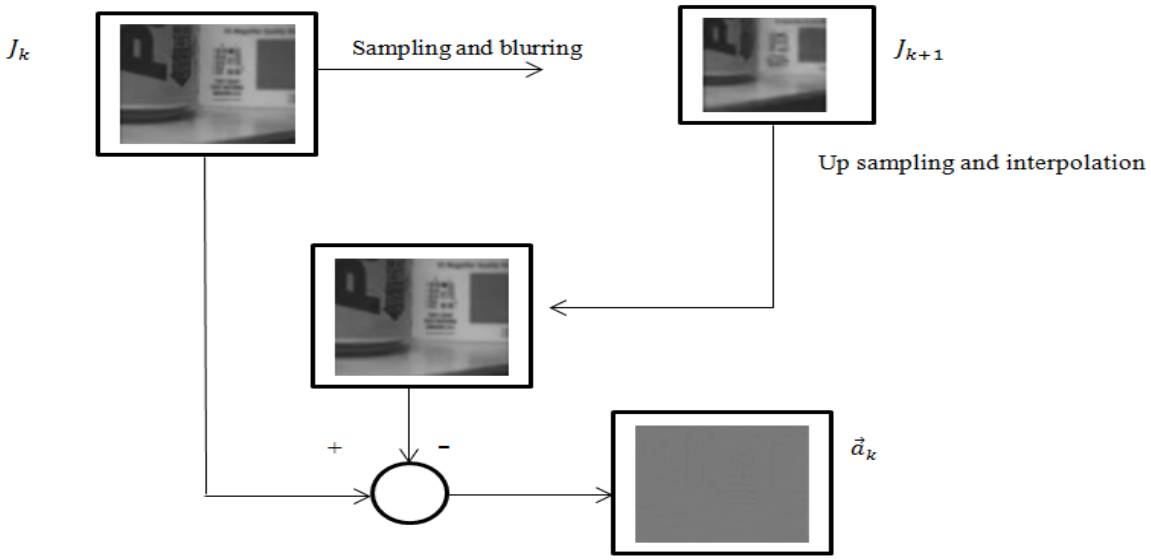

FIGURE 2. One stage of Laplacian pyramid decomposition [2].

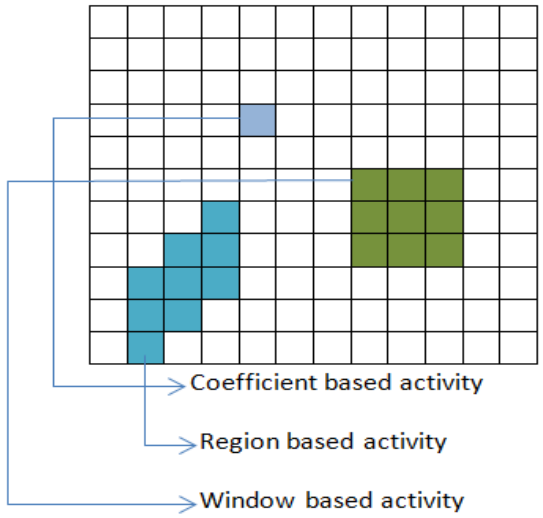

FIGURE 3. Categorisation of Activity level measurement [2].

MSD representation H_z can be given by [2], [6], [80]:

$$H_Z(\vec{x}) = W_A(\vec{x})H_A(\vec{x}) + W_B(\vec{x})H_B(\vec{x})$$

Where H_A and H_B are MSD of the source images A and B, W_A and W_B are the weights of the correlation of MSD coefficients.

4) CONSISTENCY VERIFICATION

Consistency verification aims at ensuring the similarity between the neighbouring coefficients in the composite (fused) multi-scale decomposition. For instance while constructing the fused multi-scale representation using the choose-max combining; some MSD coefficients are not described accurately by a different source image than its own neighbours. Therefore consistency verification makes sure that a composite MSD for a coefficient does not altogether come from a different source image. This can be decided using a majority filter [5].

5) AVERAGING FUSION RULE

Averaging fusion method is the most simple and basic methodology for the fusion of two source images, where the average of pixel intensities of the source images is taken in the fused image. Taking an averaging of the pixel intensity values is a way of obtaining all regions in focus. Let $P_a(i,j)$ be the pixel intensity value of a pixel in image R and $P_b(i,j)$ be the pixel intensity value of a pixel in image S. The pixel intensity values at the same corresponding positions in the source images are added and are divided by 2. The fused image can be obtained by repeating the process for all the respective pixels in the source images. The averaged value thus obtained is assigned to each pixel value of the corresponding position in the fused image. Let F be the fused image then,

$$F = \sum_{i=0}^{n} \frac{R(i,j) + S(i,j)}{2}$$

Where R(i,j) and S(i,j) are the pixel intensity values of the source images. The basic methodology of averaging fusion rule is given in Fig. 4 (a)

6) CHOOSE MAX FUSION RULE

The choose max fusion rule is one of the most trivial methods of image fusion. In choose max fusion rule instead of averaging the pixel intensity values, the pixel with maximum intensity is chosen out of the two corresponding pixels of the source images and put at the respective positions in the resultant fused image. The major advantage of this type of method is that the image does not compromise on the good

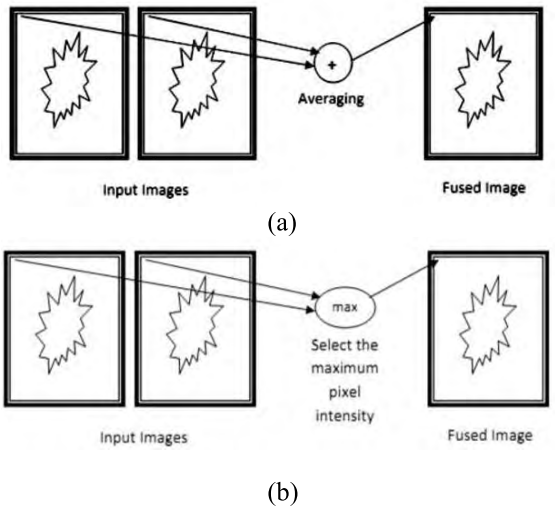

FIGURE 4. (a) Averaging Fusion Rule; (b) Choose Max Fusion Rule (For Choose Min: Select the Minimum Pixel intensity) [265].

information in the source images [2], [6]. A basic process of choose max fusion rule is demonstrated in Fig. 4(b).

7) CHOOSE MIN FUSION RULE

The choose min fusion rule is very similar to choose max rule except the selection procedure is based on the minimum pixel density of the source images. Thus, for every pixel position, the pixel of the fused image will be the pixel of the corresponding position from the input set of images having the least pixel intensity value. This method tends to keep the full information or discards in fully [2], [6].

8) CROSS-SCALE FUSION RULE

The cross scale [CS] coefficient selection fusion rule was given by Shen *et al.* [6]. The CS fusion rule was designed to transfer the information in between and within each decomposition level to achieve interscale and intrascale consistencies so that maximum amount of detailed information is preserved while exhibiting minimal number of artefacts. The basic steps in this method can be summarized as follows:

- The salient information and detailed features are transferred from the lower level to the higher level in a multi-scale representation until the approximation level is reached.
- The membership values of each of the fused coefficients in an approximation level are calculated and are passed with help of the salient information.
- Finally these memberships are used to guide the coefficient selection procedure at the detailed levels.

9) PCA BASED FUSION RULE

PCA based fusion rule is a statistical approach which aims at dimensionality reduction of multivariate data with the preservation of maximum amount of feature details. The PCA based methods help in eliminating the redundancy problems as the variables similar to each other are transformed into their one true single form. The commonly used steps in the process of PCA based fused rule is as follows [192]:

- The image matrices are represented in the form of column matrices
- Then the co-variance of each of the column vectors associated with the source image is calculated
- The diagonal values of the 2×2 co-variance vector would contain the eigen values of each of the covariance matrix
- Then by calculating the mean of the eigen values , the eigen matrices value are divided by mean to achieve normalization
- The normalized eigen vectors are multiplied with each input pixel values as weights.
- The sum of two image matrices thus obtained is the fused image matrix.

TABLE 1. Commonly used image fusion rules.

	FUSION RULES
1	Activity-level measurement based method
2	Coefficient Grouping method
3	Coefficient combining method
4	Consistency verification based methods
5	Averaging Fusion Rule
6	Choose Max fusion rule
7	Choose Min fusion rule
8	Cross scale fusion rule
9	PCA based Rule
10	Heuristic Fusion Rule

10) HEURISTIC FUSION RULE

The heuristic fusion rule is a summation based fusion rule in which the weighted coefficient values of the pixel in the fused image can be obtained with the help of the following expression;

$$F\left(\sigma^2, v\right) = \sum_{j=1}^{N} \sigma_j^2, v_i$$

where σ^2 is factor for degradation for the feature dimensions (v_i). Higher value of σ^2 gives more importance to feature space and vice-versa. The entire feature space is hence evaluated by a degrading factor which is averaged to obtain the fusion coefficients. The detailed description of this method can be found in [233].

Above mentioned description forms the basis of the various fusion strategies which gives the basic understanding of various factors responsible for the choice of the complete fusion algorithm employed in different types of image fusion.

Besides Laplacian pyramids, Pajeres and Cruz [35] gave a comprehensive view of various pyramidal fusion methods using different wavelet families. Besides wavelet transform [82], several other directionally sensitive image

transforms are Ridgelet [83], Curvelet [84]–[90], Ripplet [91]–[95], Contourlet [96]–[99], Shearlet [100]–[103], Directionlets [104] and many more. Wavelets, Counterlets, Curvelet fall under the category of multiresolution analysis whereas Laplacian pyramids fall under the domain of multi-scale analysis. The major difference between wavelet and pyramidal representation is that, in wavelets the spatial resolution of image decreases while we move from one level to the next but the image size remains constant, where as in multi-scale representation both the spatial resolution and the image size decreases as we move from one level to the next. This major difference gave MRA tools an edge over multi-scale decompositions. The concept of wavelet has been widely exploited in context of medical image fusion in [105]–[113].

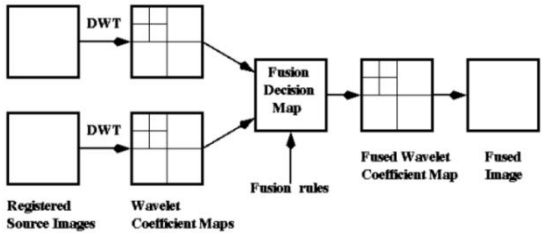

FIGURE 5. 2-D Wavelet Decomposition based fusion [35].

B. IMAGE FUSION

1) IMAGE FUSION IN TRANSFORM DOMAIN

Wavelets were designed to represent objects with 1-D singularities. The wavelet transform was used to obtain the multi-resolution analysis of the image. The image is decomposed into its lower approximation (A1) and detailed levels (H1, D1, V1) [35]. This is accomplished by using the down sampling algorithm. Once a single stage of approximation level is obtained, it is further fed as the input image in the filter banks to generate the second stage of the wavelet decomposition. After constructing the required number of decomposed levels, the wavelet coefficient maps are generated for each source images. These coefficients are fused using selected kind of fusion rule leading to the generation of the fused output image. The basic methodology of the wavelet decomposition based image fusion is illustrated in Fig. 5 [35]. The tensor product (dot) of two wavelet transforms was used to represent objects with 2-D singularities (which is the case in an image). However the wavelet showed its limitations while representing higher number of directional features and edges. The wavelet transform was isotropic in nature and was deficient of important properties like shift invariance, and multi-directionality and could not represent anisotropic features like edges and contours in images efficiently. Hence wavelet fusion based methods failed to preserve the salient features of the source images. Also the wavelet based image representations induced artefacts and noise in the fused images [97], [114].

Then to overcome the shortcomings of wavelet transform some of multi-scale geometric analysis tools like Curvelet transform based on parabolic scaling law were proposed to represent the 2D singularities. However it worked well only along smooth curves. The Curvelet transform finds its applications in many types of image fusion [115]. Besides Curvelet transform, another transform named counterlet transform was proposed which was able to capture the intrinsic geometrical features of an image. Contourlet transform comprises of a Laplacian pyramid followed by a directional filter bank. Due to its capability of capturing the curved features, the counterlet transform has been widely exploited in the domain of medical imaging [96], [116] and remote sensing applications. In a survey paper published by Shutao Li in 2011 [79] the effects of curvelet and contourlet transforms in context of image fusion has been investigated. According to the experiments conducted in [81] it was deduced that the properties like shift invariance, short length filters, and the number of decomposition levels as 4 has proven to be very effective in reducing the induction of artefacts in the final fused image. In [117] the high spectral resolution MS (multispectral) image and high spatial resolution PAN (panchromatic) image were fused using contourlet transform. The contourlet transform goes through the process of down sampling, which makes it shift variant and hence leading to Gibbs phenomena. So to overcome this limitation of contourlet transform non-sub-sampled contourlet (NSCT) was introduced which was able to represent directional features of an image more efficiently. NSCT was shift invariant.

In 2010 to sparsely represent anisotropic structures, Ripplet transform was proposed by Jun Xu [91] which is the higher order generalisation of the curvelet transform. The support parameter c and degree parameter d were introduced in ripplets which efficiently represented the arbitrarily shaped edges. In [92] Ripplet transform along with compressed sensing theory was used to fuse PAN (panchromatic) and MS (multi-spectral) images. The spatial details of PAN images were extracted by using ripplet transform and were combined with multi-spectral coefficients with the help of compressed sensing technique to obtain the final fused image. In 2011 Das et al. exploited intrinsical and geometrical features of ripplet transform to fuse CT and MRI images [118]. Besides contourlet, curvelet and ripplet other multi-scale geometric analysis tools are Ridgelets, Brushlets [119], Directionlets, Wedgelets [120], Tetrolet [121], and Bandlets. The Non-Sampled Shearlet transform (NSST) was introduced by Easley in 2009 and has proven to be a very proficient tool in context of image processing which can be witnessed in [123]. NSST was introduced by omitting the up sampling and down sampling in the Shearlet transform. NSST transforms makes use of pyramidal filter banks and sheering filters by which the coefficients of the image transform are not decimated amongst their lower levels which induces the property of shift invariance and hence caters the Gibbs phenomena very effectually. So NSST is able to give a multi-scale and multidirectional representation for edges and contours of an image.

The novel concept of NSST has been efficiently employed for image fusion in [124].

Though various MRA methods like wavelet transform and Laplacian pyramids have performed better than compressed sensing methods but their pre-defined basis functions and the fixed cut off frequencies do not allow the fusion of intrinsic and matched spatial frequency information between MS and PAN images, hence limits the applicability and accuracy of these methods.

To overcome such issues a data driven and adaptive multi-scale method i.e. empirical mode decomposition (EMD) was proposed in context of pan sharpening problems [257], [258]. EMD is a fairly adaptive method which is used for the decomposition of the non-linear and the stationary signals. EMD generates Intrinsic Mode Functions (IMF) which are finite sets of AM/FM modulated components. An IMF is a function in which the number of maxima's and the number of zero crossings are at most one and the mean of the two envelops associated with the local maxima and locally minima is zero. Using EMD, pan sharpening was performed by the fusion of the IMFs of a PAN image with those of an MS image, yielding some improvement over standard schemes [258]. However using standard EMD multi-scale methods for fusion was a bit problematic because of its multiple oscillatory modes residing in a single channel, different number of IMFs for different input channels which leads to practically meaningless fusions.

To address this problem multivariate extension of EMD i.e. MEMD was proposed to provide scale alignment (matched sets of IMFs for input data) in context of pan-sharpening problems for low resolution MS images. MEMD which is generic extension of EMD was able to overcome the limitations possessed by EMD such mode mixing and mode misalignment while providing efficient processing of signals containing multiple input channels. As shown in [259] the multivariate and data driven nature of multivariate fusion schemes have been better quantitative and qualitative results than the state of the art techniques for pan sharpening.

Another multi-scale pixel level based image fusion was proposed by Naveed *et al.* for the fusion of MS and PAN images. The potential of this scheme was demonstrated on a large data set of multi-exposure and multi-focus images. The results for this methodology outperformed the results for PCA (Principal Component Analysis), DWT (Discrete Wavelet Transform) and NSCT [260]

2) IMAGE FUSION IN SPATIAL DOMAIN

In spatial domain image fusion the image pixels in the source images are directly processed to be fused in a new image. Spatial domain pixel level image fusion can simply be obtained combining the pixel intensity values of the registered source images either in a linear or a non-linear manner. The simplest form is a weighted averaging of the registered input images to give the fused image. The spatial domain image fusion has gained popularity because of the availability of wide range of spatial domain edge recovering filters. Under category of multi-scale decomposition methods various edge preserving filters have also been constructively applied in the field of image fusion [125]–[128]. The cross bilateral filter was employed by B.K Shreyamsha in [129] to fuse many types of data sets such as multisensory and multi-focus images. A comprehensive review of image fusion techniques based categorisation amongst transform and spatial domain method is given in [130]. In 2016 Dogra *et al.* presented through various experiments that edge preserving filters like robust bilateral filter [131], weighted bilateral filter [131], [132], rolling guidance filter [133] are able to enhance the spatial characteristics and visual quality of the images in the case of osseous and vascular imagery fusion [128]. Hu *et al.* [134] coupled bilateral filter and directional filters to fuse multi-scale representations of medical and multi-exposure images. Another edge-preserving filter called guided filtering was proposed by Li et al to fuse two images together [135]. In guided filtering the images are decomposed into two layers i.e. the detail layer and the base layer resulting in extraction of large scale objects and small scale details. Gaussian and bilateral filters have been constructively employed for fusion of infrared and visible images in [136]. In [137], an improved and refined version of high pass additive filters were used to extract the textural and structural from high resolution image. These features were inserted into low resolution images and hence resulting in a highly efficient and standardised image fusion tool. The classification for image fusion methods is illustrated in Table 2.

C. NON MULTI-SCALE DECOMPOSITION BASED METHODS

The non-multi-scale decomposition methods are those which are not entirely based on multi-scale decomposition methods. In [2] Blum and Liu classified the methods other than multi-scale decomposition methods in five general categories which are namely Pixel-Level Weighted Averaging, Non-Linear methods, Estimation Theory based methods, Colour Composite Fusion and Artificial Neural Networks. According to Blum and Liu two representative methods which fall under the category of Pixel-Level Weighted Averaging are PCA (Principal Component Analysis) [138] method and adaptive weighted averaging method [139]. Some of the non-linear methods were reported by Therrien *et al.* [140]. In this non-linear method a scheme based on visual enhancement and combining of infrared and visible images which has low light was proposed. The local luminance mean of the low pass component of each of the source image was adaptively enhanced. The high pass components were modified in terms of local contrast and they were fused using weighted averaging method. The low pass components were fused using non-linear mapping. The final enhanced fused image was obtained by the direct summation of the low and the high pass components. This method of image enhancement based fusion mechanism is rather frequently targeted in current state-of-the art. These methods tend to enhance the spatial

TABLE 2. Pixel level image fusion.

Data sets	*Fundamental methodology*	*Fusion rules*	*Transforms*	*Applications*
CT,MRI,PET, SPECT, Ultrasound, mammograms, MRI, osseous, vascular, multi-Focus, infrared, visible, thermal, multi-exposure, multi-focus, Multispectral, hyperspectral, Panchromatic images	Multi-scale decomposition methods	Window [78,79] , region , cross scale [6], heuristic [142], choose-max[80,63], choose-min [6], dense-SIFT [141], activity level measurement [70], coefficient combining, pixel-level weighted averaging [139] optimization method [49], consistency verification [81,69], cross-bilateral fusion rule [129], PCA method [138],	Wavelets [35] , Laplacian pyramids [72] , counterlet [97], curvelet [87], ripplet [94] , Shearlet [102], NSCT [49], Ridgelet [93], directionlet [104], anistropic heat diffusion method [50], log-Gabor transform [49], Edge preserving filter methods [127,135], high pass filter additive [137], empirical mode decomposition methods [259]	Tumor detection, brain diagnosis, lung cancer detection, detection of cerebral iron deposits, abdomen studies, metastasis detection, tinnitus, vascular diseases, sarcoma, toxoplasmosis, astrocytoma, HDR imaging, remote sensing, military surveillance, R& D, concealed weapon detection, spectroscopy
	Non-multiscale decomposition methods			
	Artificial neural networks & fuzzy logic [154,155]	Wavelet neural networks [176], clustering neural networks [158], fuzzy neural network [166], multi-wavelet coupled neural network [164], un-decimated neural network, image fuzzification and defuzzification [174], neuro-fuzzy networks [50]	Wavelet packets, DWT, decimated and undecimated wavelet transforms, MRA tools	
	Sparse representation	Weighted average, choose-max, sparse coefficient substation method, activity level measurement, window based	Orthogonal matching pursuit [178], over complete dictionaries [186], spatial detailing dictionary[187], spectral detailing dictionary [188]	
	Methods in other domains (non-transforms)	Weighted average, component substitution [198], activity level measurement based method [70], region based activity level measurement, block based activity level measurement [197]	IHS [189], PCA[192], Gram Schmidt [193], ICA [191], Graph cuts, random walker	
	Hybrid methods	Component substitution [49], Weighted average, choose-max, window based activity level measurement, coefficient substation-weighted average	IHS-wavelet [143], SVM [208], IHS-Curvelet [201], PCA-wavelet [205], sparse representation-probability theory methods [184], MRF [217],	

consistency and visual perception of the local and the non-local features in the final fused image. These techniques have proved to obtain encouraging results in the last decade [141]–[143]. In [144] the authors reviewed a class of image fusion methods based on maximum a posterior (MAP). These methods are based on the image formation models which describes a relationship between the underlying true image and the source images. These methods are popularly called estimation theory methods which comprises of two prime components which are the prior model and the image formation model. A generalised approach to the usage of locally affine transformation with the help of non-Gaussian distri-

butions was presented in [145]. In [146] the image fusion methods based on random walker based optimization were further improvised by calculating the optimal fusion weights derived from MAP in the hierarchy based multivariate conditional Gaussian random field model. Another fascinating approaches employing estimation theory which are based on Markov random field can be found in [147] and [148]. The process of image fusion which involves the fusion of the input image with the coloured domain to obtain a less true colour representation of the fused image is called colour composite fusion. A lot of work based on coloured image fusion can be found in [149]–[151].

1) ARTIFICIAL NEURAL NETWORKS

ANN (Artificial neural networks) is an idea inspired from the biological learning of the neural networks via input sources to process various features parameters which are finally capable of making global decisions. The models based on artificial networks are fed an input training set for identification of the parameters (weights) related to the networks. The major advantage of the artificial neural networks which has made them very popular in the recent years is their ability to infer, analyse and also predict the information from the given data set. This advantage laid off the whole load of the mathematical complexity. Pulse coupled neural networks [152]–[154] and multi-layered perceptron neural networks [155] are the two major types of neural networks which have been frequently used for image fusion. The capacity of the neural networks to train themselves adaptively according to the changes in data sets has enabled them to be very useful for several applications for instance data fusion [156]–[158] for medical diagnostics [159]–[161] and natural computing methods [162].

Zhang *et al.* [163] trained the pulse coupled neural networks to estimate the weights with the local sparse features as inputs. These inputs were calculated by decomposing the source images in sparse matrices and principal component matrices. In spite of the general advantages of advanced training ability and lower mathematical complexity the robustness of the artificial neural networks is majorly limited by the region of convergence of the training algorithm and the quality of the training data set. A lot of improved neural network based image fusion techniques have been reported in the recent literature [164] to improve the performance of ANN by uplifting the quality of the training data set. Besides ANN, the neuro-fuzzy logics are widely applied both as feature based operator or a decision based operator for fusion of data sets aiding medical imaging diagnostics [165]–[168]. The various applications of fuzzy logic in image fusion are deep brain stimulation process [169], image retrieval [170], [171], multimodal image fusion [172], natural computation methods [162], genetical expression [173] and multi-sensor image fusion [174]. The improvisation in fuzzy logic image fusion methods is based on the type of fuzzy sets and membership functions. The fuzzy neural networks are frequently combined with probabilistic approaches to enhance their strength such as fuzzy probability in [175] and neuro-fuzzy wavelet in [176].

2) SPARSE REPRESENTATION BASED METHODS

One of the extremely important and active classes of image fusion methods is sparse representation based methods. Sparse representation based methods have gained significant attention in the recent years due to various successful applications in the field of image processing and computer vision. The sparse representation based methods are able to achieve more stable and meaningful representation because of the availability of the over complete dictionaries which forms a training set of the source images for the fusion. Unlike traditional Multi-scale transforms (MST) based methods they do not use presume fixed basis function. In addition, they are less susceptible to mis-registration among the source images, thus facilitating the practical applications. In sparse representation the images can be described sparsely by a linear combinations of the atoms derived from over complete dictionaries. The main property of the sparse representation (SR) based methods is that a very less number of non-zero elements (sparse weighted coefficients) are required to describe the salient features of the image.

A sparse representation based multi-focus image fusion method is proposed in [177]. In this method the source images are represented in the form of sparse coefficients with help of over-complete dictionaries and then these sparse coefficients are fused with the help of choose max fusion strategy. Finally the fused image is reconstructed from the fused sparse coefficients with the help of the dictionary. This method is able to overcome the shift variance problem with the help of a sliding window approach and is also able to resolve the image restoration problems. The proposed method is able to outperform various existing image fusion methods [177].

In a work given in [178] an orthogonal matching pursuit (OMP) based algorithm was applied to obtain the spare coefficients from the source images. The distribution of the non-zero elements has shown to exhibit some special structures of images. In a fusion algorithm presented by Li *et al.* [179], the input images are partitioned into overlapping image patches. The corresponding sparse coefficients are obtained using over complete dictionaries. And finally the fused image is constructed from the dictionary and coefficients are fused using choose max fusion strategy. To take ahead the work presented in [177] Yang and Li utilized simultaneous OMP to obtain the patches from the multiple source images on the same dictionary [180]. This technique helps to exploit the correlation amongst the pixels and places the non-zero coefficients of both the source images at same locations. Some of the other important works based on image fusion using sparse representation methods are given in [181]–[185]. While constructing the fused images using sparse representation, over complete dictionaries plays a major role. There are two universal methods stated in literature to construct the dictionaries namely mathematical models (discrete cosine transform, curvelets and wavelets)

and methods based on example learning (K-SVD and method optimal direction) [186]. However dictionaries based on a single mathematical model has poor representation for natural images. Therefore the focus of the researchers has shifted on constructing hybrid and over complete dictionaries which can reflect various image structures and are learned from a large set of training set similar to the input images [187]. Wang *et al.* [188] build the spatial detailing dictionary and spectral dictionary to fuse multi-spectral and panchromatic images. For representation models, the traditional SR (Sparse representation model is the most popular in image fusion. Extensions, such ASR (Adaptive Sparse Representation), GSR (Group Sparse representation), NNSR (Non Negative Sparse Representation), JSR (Joint Sparse Representation), and RSR (Robust Sparse Representation model, have also been applied in image fusion.

Most of the SR based methods are employed in the form of patch based way. This necessitates the use of a sliding window which increases the loss of the spatial information and increases the computational complexity. Integration of some local consistency prior into these SR models during the sparse coding phase for each image patch could be effective solution to this problem [267].

Most of the sparse representation based image fusion methods exploit traditional fusion strategies such as choose max and window based activity level measurement, weighted average based coefficient combining and substitution of sparse coefficients. Therefore designing of more advanced and adaptive fusion strategies well-suited for sparse representation based methods could be another open challenge for the researchers.

3) METHODS IN OTHER DOMAINS

There are several other types fusion methods based on dimensionality reduction algorithms e.g. Intensity-Hue-Saturation [189]–[190] Independent Component Analysis [191] and PCA [192] based methods and Gram Schmidt [193] transform method. These techniques are often used in combination with wavelet transform and are based on feature processing and dimensionality reduction. A hybrid fusion approach by Jiang *et al.* [194] is presented which uses morphological component analysis to decompose the source images and sparse representation based methods to fuse the decomposed coefficients for pan sharpening problems. The methods which aims at combing high spectral resolution images and high spatial resolution panchromatic images popularly called as pan-sharpening problem. Another straight forward approach to fuse two images together could be to take each pixel in the fused image as the weighted average of the respective pixels in the source images. The activity level measurements of pixels determine the corresponding weights attached to the pixel. Li *et al.* [195] to make full use of the spatial context information, fragmented the input images in uniform blocks where spatial frequency of the each block is maximized. However these kinds of approaches may induce block artefacts on the boundaries of the objects [196], [197]. Besides opting block-wise fusion another idea could be using region based image methods. However these methods fuse regions with irregular shapes obtained by image segmentation. These methods are limited by relying heavily on image segmentation which is another challenging problem in image processing. Apart from block formation based and image segmentation based methods other class of methods which exploits the spatial correlation amongst the pixels is presented in [198].

Another class of image fusion methods is graph cut algorithms which are based on the discrete optimization methods. These methods find their applications in computer vision, image segmentation, stereo vision and image restoration. The graph cut methods are employed for object recognition by segmenting planar surfaces from depth images. The graph cut based segmentation algorithm uses depth and intensity values as inputs to be combined. The graph cut methods were exploited in context on spine image fusion in [268]. In this method both bone and soft tissues contained in CT and MR images were combined in a single image to facilitate the patient diagnosis. This method formulates a discrete multi-label optimization problem which is solved via graph cut methods. The proposed methodology in [268] is a striking balance of three competing terms:

1) A squared error which gives preference to strong MR edges
2) A squared error which gives preference to the strong CT edges
3) A prior, favouring smooth solution by encouraging neighbouring pixels to have similar fused-image values.These methods have shown to give promising results and global solutions while exhibiting minimal amount of pixilation artefacts.

4) HYBRID METHODS

Though plethora of multi-scale and non-multi-scale methods has been devised so far, the combination of methods from different domains has proved to be very competent in the case of image fusion. Hybrid methods harness the attributes and advantages of diversified methods which are complementary to each other. The conglomeration of CS (compressed sensing) and MRA (multiresolution analysis) has been successfully applied in context of image fusion [199]. In this work an advanced ICA (Independent Component Analysis) based fusion method which employs wavelet decomposition technique to extract the detailed features of PAN is given. The major advantage of CS based fusion is that it can greatly lessen the processing time along higher quality fusion results with lesser non-zero coefficients.

Though the compressed sensing based fusion algorithms reduces computational complexity and processing time by using fewer non-zero coefficients, while directly fusing compressed sensing coefficients may bring uncertain results and can lead to the occurrence of block artefacts. Therefore the images features are first extracted using ICA-Wavelet based method. It has been also observed that using single

fusion rules can result in high reconstruction error and poor fidelity. In a work presented in [200] the low pass and high pass coefficients are fused separately using sparse representation and activity level measurement fusion technique. The output fused image is obtained in the final step using inverse multi-scale transform. The authors have proved that this method is superior in performance to individual sparse representation or multi-scale transform methods. A hybrid method combining IHS (Intensity Hue Transformation) and Curvelet transform is contrasted with wavelet a trous algorithm, wavelet, curvelet and ridgelet transform in [201]. A multimodal image fusion method based on IHS and PCA has shown to preserve functional information and spatial feature without distortion in colour [202].

Various wavelet based methods have been presented in [203]. In these methods the higher frequency detailed coefficients are extracted from PAN image which have high spatial resolution and combined with MS images providing higher amount of spectral information. Similarly a fusion method for HS and MS images based on sparse representation has been introduced in [204]. This method based on sparse matrix factorisation comprised of two stages. The first stage is to learn the low spatial resolution data from a spectral dictionary with true signatures. In second stage the high resolution spatial and spectral data is extracted from the learned spectral dictionary.

While discussing PCA based fusion methods it can be said that though they are able to provide higher spatial resolution but they can lead to more serious distortion based errors in the spectral characteristics. On the other hand the wavelet transformation when used alone is able to preserve the spatial information but results in lack good spatial representation. To counter such limitations a combined technique based on PCA transformation and wavelet decomposition has been given in [205]. Besides these the grouping of wavelet transform with complex counterlet transform has shown to give robust image fusion results as compared to individual counterlet or wavelet transforms [206], [207]. Liu *et al.* [207] first decomposed the source images using multi-scale decomposition methods. The high frequency components are fused using the traditional fusion rules whereas the low frequency components were fused using the sparse representation based methods.

Another class of image fusion methods is SVM (Support Vector Machine) based techniques [208]. These techniques are kernel based techniques which possess strong control over feature space and are parameter and data driven. SVM has proved to be a strong tool in image processing because of its strong ability of rejecting the outliers and has several applications in cancer diagnosis [209], tumor segmentation [210] and content based image retrieval [211]. In image fusion the suitability of various approaches in different applications is dependent on type of data to be fused and the spatial and the spectral quality of the source images. In [212] a comparison has been drawn amongst PCA, Wavelet, Local mean matching, Local mean and variance matching, Brovey transform, IHS, modified IHS and multiplicative fusion techniques on QuickBird data. Another category of image fusion methods is model based methods which can be closely related to probalisitic methods. In [213] a fast and multi-band image fusion method is proposed which constructs the likelihoods of the various observations. In this algorithm the solution of the Sylvester equation leads to the minimization of the likelihoods. Further by utilizing the properties of the down-sampling and circulant matrices a closed solution of the Sylvester equation solving the fusion problem is obtained. This method can be advanced by using the Bayes estimator to provide the prior information of the fusion problem. Going by the similar lines a hierarchy based Bayesian model for the fusion of multiple band images with several spatial and spectral resolutions is given in [214]. The posterior distribution is obtained using Hamiltonian Monte Carlo algorithm and prior distribution are estimated from geometrical considerations. The MRF (Markov random Field) theory based methods top the chart in model based methods. In a work given by Golipur et al. in 2016, MRF based theory provides the basis to form contextual constraints models in visual interpretation and processing [215]. In [216] the technique for extracting the contextual constraints using MRF models has been induced to design two fusion models. The first algorithm is applicable for multi-scale decomposition based fusion approaches and second is only applicable for non-multi-scale decomposition based fused methods. Various another MRF based fusion models have been proposed in [217] and [218]. The concept of random walks has also been widely applied in multi-focus and multi-exposure image fusion. In [269] a generalized random walk framework is employed to calculate an optimal solution which takes into consideration both the local contrast and colour consistency measures. This method is a probabilistic model based fusion technique which is utilized for multi-exposure image fusion.

Another application based multi-focus image fusion is done with the help of random walks on graphs [270]. This work exploits random walks on graphs and its relationship to multi-focus image fusion problems. The proposed method has been able to overcome the weaknesses possessed by pixel-based methods and belongs to the spatial domain category. This method is employed by the evaluation of the focus areas in a local sense and identifies the nodes corresponding to the consistency of the nodes in a global manner. A fully connected graph is created to represent the local and global characteristics by evaluation of several feature sets which are based on colour consistency and focus measure. The random walk graphs are utilized to compute the weighting factor for the shallow depth-of-field input image. The fused image so obtained has a greater field of depth than input images. The normalization weighting method is able to avoid the over smoothing of the fused image.

Various transforms have their advantages as well as their limitations. On one hand the multi-scale transform based image fusion methods can efficiently extract spatial structures at different scales but they do not represent the

low-intensity components of the images sparsely and these low intensity components can contain the main energy of the signal. On the other hand the sparse representations based method could provide better description of the detailed features and edges of the images using dictionary learning; they tend fail at reconstructing the small-scale details of the source images. Besides if PCA and IHS based method are effective then they cannot be generalised for different types of source images such as multi-exposure and multi-focus image fusion. Therefore there a lot of work is carried out on hybrid methods. These hybrid approaches tend to reduce noise and artefacts by enhancing the source images prior to fusion and these methods have found applications in diverse domains [219]–[224].

III. FEATURE LEVEL IMAGE FUSION

Feature level image fusion is one level higher than the pixel level image fusion as it deals with higher level processing of the data. This is accomplished by firstly extracting the features and then fusing these features using advanced techniques. For instance one method of employing feature level image fusion is region based fusion scheme. Image segmentation plays a vital role in feature level image fusion as it is used to generate a set of regions. The set of regions can be used to calculate various region features or properties. The properties corresponding to features which depend on their environment such as extent, shape and neighbourhood are extracted from the original source images. Then the object possessing the similar properties are linked to each other and then fused for further analysis. However feature level image fusion is sometimes rather tricky when feature sets are derived from varied data sources and algorithms [48]. In the following section some of the feature level image fusion methods will be discussed.

In [266] a multi-focus image fusion method is given by Hui Li et al. based on the feature extraction method.

In this method the multi-focus image fusion is achieved with the help of sparse feature matrix decomposition and morphological filtering. Firstly the source images are decomposed into their sparse feature matrices. Then these sparse feature matrices are weighted with salient features to obtain the temporary matrices for the multi-focus source images. Then the concept of morphological filtering is applied to extract the bright and the dark regions of the source images. A base image is formed by weighing the source images. The final fused image is obtained by importing the extracted features on to this base image.

In [251] a study is presented which introduces three image fusion techniques based on PCA (Principal Component Analysis) based feature level fusion, edge based fusion and segment based fusion. This study is briefly discussed to present an insight to the feature level image fusion. In segment based fusion an idea was developed which aimed at preserving the spectral characteristics of the MS (Multispectral Image). The proposed methodology was based on spatial domain filtering coupled along with IHS (Intensity Hue Saturation) transform. The problem formation was that the PAN (Panchromatic) image should be able to sharpen the MS image without the addition of any extra grey level pixel intensity data to the spectral coefficients of the MS image. This was done by separating the spatial and the colour information and then adaptively enhancing the spatial content of the image. The intensity segment (component) of the MS image is extracted using low pass filter and is fused with high resolution PAN image using the high pass filtering [251].

In PCA based feature level fusion the features from the original image are projected in the form of their principal components and are stacked in accordance to their variance values. Hence the features of an image are displayed as a linear combination of the feature values in an uncorrelated manner. Finally the fusion process is done by extracting and fusing only those features which constitute a substantial amount of information.

The edge detection based image fusion is one of the most common types of feature level image fusion. In [251] the gradient based information is extracted from the source images using the first order derivatives and by employing edge detection filters i.e. Roberts, Prewitt and Sobel edge detectors. These filters extract the relevant edges from the source images. The extracted edges are then added to the low pass filtered intensity values of the MS image. Then the feature level fused image is obtained using the inverse transformation. The quantitative evaluation metrics used in this study are standard deviation, entropy, signal to noise ratio, deviation index, correlation coefficient, and normalized root mean square error. In all the authors have concluded that the segment based fusion technique work efficiently for the beat representation of the spectral and the spatial information of the remote sensing images [251].

The subjective evaluation results for the segment based fusion, Edge based fusion and decision based fusion are depicted below in Fig. 6 [251]

The feature level image fusion aims at fusion of specific types of features from the source images rather than all the image features as in pixel level image fusion. Another example of feature level image fusion can be seen in [252] where Dual Tree Complex Wavelet Transform (DT-CWT) has been employed to perform feature level image fusion. The DT-CWT along with watershed transform is used to produce a region map of the segmented features of the input images. The segmentation map is obtained by joint segmentation of the input images. With the help of the segmentation mapping the significant features like standard deviation are calculated which are fused with the help of wavelet based fusion method.

The feature level image fusion is usually employed when the fused image has to be synthesized to perceive specific features of the source image more accurately. Feature level image fusion is also used to avoid redundant data fusion and blurring of the important edge information.

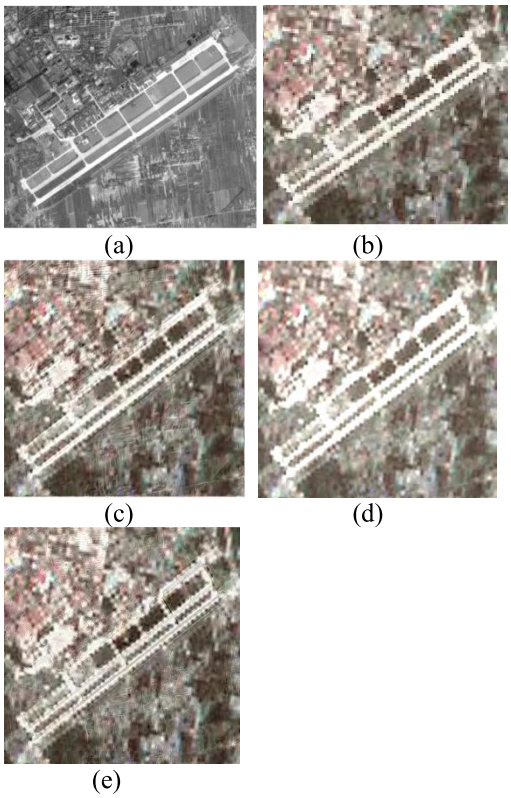

FIGURE 6. (a) PAN image; (b) MS image; (c) segment fusion; (d) PCA based fusion; (e) edge fusion [251].

IV. DECISION LEVEL IMAGE FUSION

Decision level image fusion is also called interpretation level or symbol level image fusion and is known as the highest processing stage in image fusion. In decision level fusion locally classified data from several input images is combined to determine the final decision. Each of the individual source images has to undergo some pre-processing for the extraction of the information. Then decision rules with varied degree of confidence are exploited to combine the information extracted to realize a better understanding of the objects under observation.

Decision level image fusion finds its applications in varied fields such as finger print verification, biometrics and several other remote sensing applications. Besides this decision level image fusion is also used in parallel and distributed processing systems [48].

A decision level fusion scheme for finger print verification is considered in [7]. The scheme specifically stresses upon the significance of the classifier selection while the combination of extracted features. The decision level image fusion classifier employed in [7] uses the Neyman Pearson optimal rule. The each of the classifier selects their own representation scheme and produces a varied confidence value as its output. The scheme is proposed to fabricate a multi-modal biometric design system which processes the data from multiple numbers of finger print matchers. The overall accuracy of the system design was upto the mark due to the aggregation of the multiple finger matches.

As compared to pixel level image fusion the literature available or the work done in the field of decision level image fusion is sparse. This can be attributed to the fact that the decision level image fusion is quite application sensitive.

In the review paper given by Ghassemian and Hassan [48] some of the significant fusion methods employed in various applications are Bayesian Interface, Dempster Shaft methods, rank based methods and voting. Each of these methods has their own advantages and drawbacks.

The Bayesian method used in decision level image fusion causes the error and complexity in the measurement values of the posterior probabilities and this method does not take into account the uncertainty factor. The output measurement values by this method become highly unstable when the number of unknown values exceeds the number of known values. Some of the drawbacks of this method could be overcome by the Dempster Shaft method as it can be employed without the prior information of the probability distributions [48].

In [253] the joint measures method was introduced as a powerful method which was able to cater any type of decision level fusion problem where there could be an uncertainty between the clear and uncertain local classifier results. The method was employed to devise a performance enhanced fusion scheme for data obtained in varied spectral bands such as microwave, thermal, infrared and visible region. The method was able to model the classifier performance by introducing the plausibility and correctness measures.

In another study reported in [254] the decision level image fusion is used for the purpose of object recognition. Firstly each of the source images are analysed for individual object oriented view and then finally by forming the contextual scene information as the basis the classified objects are combined together via decision based fusion strategy. The proposed methodology is tested on World View Satellite images. The results for the source data sets and the fused images given in [254] are depicted in the figure 7 below. It depicts the Object-based image analysis on individual WV-2 satellite images and final decision-level fusion object recognition results.

V. PERFORMANCE EVALUATION METRICS

In the literature various evaluations metrics to measure the performance of different image fusion techniques have been proposed. These metrics are broadly classified in two main categories i.e. classical and gradient based methods [129]. The classical methods can be given as follows: [225], [226]

Assuming two source images to be fused as R and S:

1) Average Pixel Intensity or Mean gives the measurement of the index of the contrast and is given by $API = \vec{H} = \frac{\sum_{i=1}^{l}\sum_{j=1}^{m} h(i,j)}{l \times m}$ where h (i, j) is the pixel intensity at (i, j) and $l \times$ m is the size of the image.
2) Information Symmetry also known as Fusion Symmetry (FS) shows the level of symmetry of the fused image with respect to the source images and can be given as $FS = 2 - \left| \frac{MI_{RH}}{MI} - 0.5 \right|$

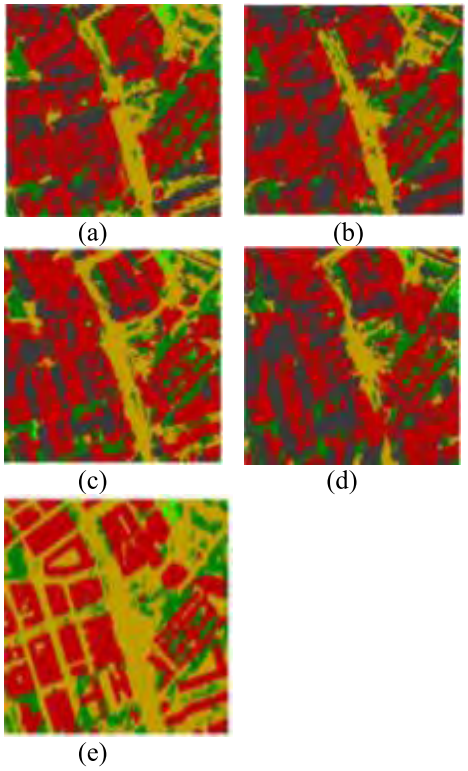

FIGURE 7. Results on the WorldView-2 dataset (a-d) Object-based image analysis on individual WV-2 satellite images; (e) Final decision-level fusion object recognition results [254].

3) Average Gradient (AG) computes a degree of sharpness and clarity and can be given as

$$AG = \frac{\sum_i \sum_j \left(h\left(i,j\right) - h\left(i+1,j\right)^2 + h\left(i,j\right) - h\left(i,j+1\right)^2\right)^{\frac{1}{2}}}{lm}$$

4) Mutual information (MI) calculates the overall correlated or mutual information between the fused image and the source image and can be given as $MI = MI_{RH} + MI_{SH}$
5) Standard Deviation (SD), which reflects the spread of the data in the entire image and is given as $SD = \sqrt{\frac{\sum_{i=1}^{l}\sum_{j=1}^{m}\left(h(i,j)-\bar{H}\right)^2}{lm}}$
6) Entropy measures the amount of information present in the image and is given by $E = -\sum_{k=0}^{255} \rho_k log_2\left(\rho_k\right)$, where ρ_k is the probability of intensity value k in an 8-bit image.
7) Spatial Frequency (SF) calculates the overall information or the activity level in the regions of an image and is measured as $SF = \sqrt{CF^2 + DF^2}$ where $CF = \sqrt{\frac{\sum_i \sum_j h(i,j) - h(i,j-1)^2}{lm}}$ and

$$DF = \sqrt{\frac{\sum_i \sum_j h\left(i,j\right) - h\left(i-1,j\right)^2}{lm}}$$

8) Correlation Coefficient (CC) computes a relevance of fused image to the source images and can be given as $CC = \frac{\left(r_{RF} + r_{RF}\right)}{2}$.
9) Root Mean Square Error (RMSE) depicts the amount of distortion of the fused image as compared to original reference image and is given as

$$RMSE = \sqrt{\frac{1}{LM}\sum_{i=1}^{L}\sum_{j=1}^{M} K_r\left(i,j\right) - K_f\left(i,j\right)}$$

Where $K_r\left(i,j\right)$ and $K_f\left(i,j\right)$ are the image pixel values of the reference and the fused image respectively [255].
10) The Erreur Relative Globale Adimensionelle de Synthese (ERGAS) is composed by the sum of the root mean squared error values is another objective evaluation metric which is used in remote sensing PAN sharpening applications. The formula for ERGAS can be given as

$$ERGAS = 100\frac{M}{N}\sqrt{\frac{1}{N_p}\sum_{i=1}^{N_p}\frac{RMSE(band_i)^2}{MS_i^2}}$$

Where M and N display the size of the PAN and MS images, N_p is the total number of pixels in the fused image. MS_i is the mean radiance value of the MS image for the i^{th} band [255].
11) Universal Image Quality Index (Q) is a metric which is used to evaluate the quality of the monochrome images as is given as

$$Q\left(i,j\right) = \frac{\sigma_{ij}}{\sigma_i\sigma_j} \cdot \frac{2\overline{IJ}}{I^2 + J^2} \cdot \frac{2\sigma_i^2\sigma_j^2}{\sigma_i^2 + \sigma_j^2}$$

where σ_{ij} is the sample covariance, $\bar{I}$ is the sample mean of I. The value of Q varies between -1 and 1. Q4 vector index is the vector extension of Q-index and is usually employed in examples with datasets having four spectral bands for instance in remote sensing applications. The Q4 index can take up values from 0 to 1 [255].

Now besides these above mentioned classical methods there are several other unique gradient based performance metrics which do not require a reference image. These metrics give in-depth analysis of the fusion process and more widely used in the present scenario. These parameters are symbolically and mathematically defined as follows [129], [226], [227]:

$Q^{RS/F}$ = Total information transferred from the source images to the fused image

$L^{RS/F}$ = Total loss of the information and

$N^{RS/F}$ = Noise or artefacts which occur in the fused image due to the fusion process. In fact these three parameters total fusion performance, fusion loss and fusion artefacts are complimentary to each other and will sum up to unity.

$$Q^{RS/F} + L^{RS/F} + N^{RS/F} = 1$$

A modified version of these parameters is given in [246] which measures the fusion artefacts as

$$N_m^{RS/F} = \frac{\sum_{\forall i}\sum_{\forall j} RM_{i,j}[\left(1 - Q_{i,j}^{RF}\right) w_{i,j}^{R} + (1 - Q_{i,j}^{SF} w_{i,j}^{S}]}{\sum_{\forall i}\sum_{\forall j} w_{i,j}^{R} + w_{i,j}^{S}}$$

where, $RM_{i,j} = \begin{cases} 1, g_{i,j}^{F} > g_{i,j}^{R} \text{ and } g_{i,j}^{F} > g_{i,j}^{S} \\ 0, \text{otherwise} \end{cases}$, indicates those location of fusion artefacts where fusion gradients are stronger than input.

$g_{i,j}^{R}$, $g_{i,j}^{R}$ and $g_{i,j}^{R}$ are the edge strengths of R, S and F respectively.

$Q_{i,j}^{RF}$ and $Q_{i,j}^{SF}$ are the estimates of the gradient information preservation of the source images R and S respectively.

$w_{i,j}^{R}$ and $w_{i,j}^{R}$ are the weights of the source images R and S.

Now $Q^{RS/F}$ which gives the measure of edge transfer rate from source images to the fused image is given as

$$Q^{RS/F} = \frac{\sum_{i=1}^{l}\sum_{j=1}^{m} Q^{RF}(i,j)\, w_i(i,j) + Q^{SF}(i,j)\, w_j(i,j)}{\sum_{i=1}^{L}\sum_{j=1}^{M} w_R(i,j) + w_S(i,j)}$$

Q^{RF} and Q^{SF} are edge preservation values which are weighted by $w_R(i,j)$ and $w_S(i,j)$ where i and j denotes the location of the pixels.

Therefore $L^{RS/F}$ the loss of information can be given as $1 - (N_m^{RS/F} + Q^{RS/F})$.

More detailed analysis of these various performance comparison metrics in context of image fusion can be found in [226]

VI. RECENT TRENDS IN IMAGE FUSION

Analysing the gradual and progressive growth in the image fusion methods some of the important and remarkable techniques irrespective of the type of fusion methods they belong to and which have proposed in the last six years are reviewed. A recent review of image fusion techniques on the state of art methods is presented in the following paragraphs:

In 2011 Jing and Chen proposed a bilateral filter based method to obtain a multifocus image with enhanced gradient based information in the image. Multifocus image fusion is done with an aim to combine multiple images with varied focii for enhancing the comprehension of the scene. In this work a bilateral sharpness criterion is proposed to exploit the phase coherence and detail strengths of the image. This is achieved by using the gradient information of the images. This technique is able to outperform the existing techniques in terms of sharpness criterion measure. However the scope of this work has been limited to spatial domain methods and the noises prevalent in the fused image are neglected [229].

In a work proposed by Li *et al.* [230] the problem of fusion of multi-focus images in dynamic scenes has been addressed. The issue is handled with the help of image matting. Through image matting the authors combined the focus information and integrated the nearby correlated pixels to obtain precise fusion results. The methodology of this work consists of obtaining segments of source images through morphological filtering and is fed as the input of the image matting. The image matting technique is further used to obtain the focussed region of each source image and finally fused together to obtain a multi-focus image. This approach forwards the focus information to image matting to find the focussed region. Matting enables the exploitation of full correlation amongst the pixels. However the loss of information and occurrence of artefacts has not been taken into account in context of this article.

Srinivas Koduri [231] in 2012 proposed the multisensory fusion with singular value decomposition. Satellite imaging consists of data at varied radiometric and spatial resolutions due to limited transmission bandwidth and other technical constraints. The study has displayed the outstanding performance of SVD (Singular Value Decomposition) for panchromatic and multispectral data. However the computational complexity involved in implementation of SVD is very high.

In [232] again in context of multi-focus image fusion, Jing and Chen in the year 2012 proposed a new statistical sharpness measure by exploiting the observation of varying marginal distribution of wavelet coefficients for different images with different focus. The distribution of wavelet coefficients is exploited using a locally adaptive Laplacian mixture model. The image fusion is then performed in the wavelet domain using the sharpness measure. The basic wavelet methods have been used in this work which provides lesser directional sensitivity.

In 2013 in order to make full use of spatial consistency in base and detail layers, Li *et al.* [135] proposed an effective fusion method to create a highly informative fused image by using guided filtered weighted average techniques. The method consists of two scale decomposition into layers containing higher scale variations (base layer) and layer containing small scale variation (detail layer). The guided filter is used in a novel way to exploit correlations amongst neighbouring pixels for filter weight optimization. The methodology is computationally efficient making it viable for real applications. However the performance of the guide filtering can be further improved by optimizing the choice of filter parameters.

Shen *et al.* [6] proposed a method for 3D medical image fusion. Combined analysis of the medical data received from various imaging modalities has become a common clinical practise and has increasing importance in the medical community. The author has proposed a cross scale fusion rule for fusion of volumetric medical images exploiting multi-scale decomposition considering both intrascale and interscale consistencies. An optimal number of multi-scale representations coefficients are collected by using the neighbourhood information. The element of colour fusion has also been added to the present work. This work can be set as a paradigm of 4D medical fusions. However the noise and artefacts emerged in the fused image are neglected.

In 2013, B.K Shreyamsha [129] exploited the attributes of cross bilateral filter to present a pixel level based image fusion. Cross bilateral filter (CBF) constructs weights which takes into account both geometric closeness of the neighbouring pixel and grey level similarities. The underlying idea of CBF to use one image to design the filter kernels of another image and vice versa has made into use efficiently to fuse multi-focus and multisensory images. Besides the evaluation of the proposed algorithm has been large number of objective metrics e.g. Average Pixel Intensity, Standard deviation, Average gradient, Entropy, Mutual Information, Fusion Symmetry, Correlation Coefficient, and Spatial Frequency. The author has reported the highest fusion rate or information travel rate so far. However the CBF rule does not work well on dissimilar images as reported in [142].

In 2014 targeting the preservation of low level features in terms of spatial consistency GRWT (Generalized Reisz Wavelet transform) is used for fusing multimodality images. The GRWT combined with heuristic fusion model based on optimal parameterization fusion model and structural information has been used to capture the directional image structures. The method has been performed to preserve the structural information effectively and induce the spatial consistency in the multimodal fused image [233]. However the application of the proposed algorithm is limited to specific type of data set and cannot be generalised for all types of data sets.

In 2014 an effective feature extraction method for the hyperspectral images based on image fusion and recursive filtering (IFRF) was proposed. The underlying principle has been the partitioning of hyper-spectral images into multiple subsets of adjacent sub bands falling in the domain of hyper spectrum. Then by employing the averaging fusion rule each sub bands are fused together. Further the fused bands are processed with recursive filtering to extract desired features. The method proposed works efficiently in terms of computational efficiency and classification accuracy. However in spite of high classification accuracy obtained in this algorithm, the choice of parameters and number of features are not exhaustive. This is due to the large number of parameters involved in the optimization of filtering [234].

In 2015 dense scale invariant feature transform (SIFT), was used to fuse multi-focus and multisensory images. The efficiency of dense SIFT is motivated by the fact that for each source images three weighted terms namely spatial consistency, exposure quality and local contrast are used. The algorithm is adopted to remove ghosting artefacts when the scene captured is dynamic with moving objects. The algorithm works well to match mis-registered pixels between multiple source images to improve the quality of the fused image [235], [236]. However the information transfer rate is not competitive with state of art fusion techniques.

In 2016 in order to achieve a higher information transfer rate Dogra *et al.* [141] proposed a cascaded scheme to fuse DSA and mask images. The various stages of the technique comprised of different transform domain methods. The edge information present in the source images were enhanced prior to fusion. The final outcome is an innovative step by step processing of DSA images, mask and contrast before fusion with recently developed images transforms and high pass filters. Finally the DSA and mask images are fused using dense SIFT fusion algorithm. The information transfer rate achieved was as high as 0.8475.

In 2016 Yu Liu applied convolutional sparse representation (CSR), a signal decomposition model in context of image fusion. The CSR method was able to overcome the limitations possessed by sparse representation methods i.e. their compromised ability in detail preservation and high misregistration sensitivity. This image fusion technique designed in CSR based image fusion framework where the source image is decomposed into a detail layer and a base layer has outperformed several state-of-the-art-sparse representation methods [237].

In 2017 focusing on two crucial factors in the fusion of images i.e. measurement of activity level and choice of fusion rule Yu Liu introduced convolutional neural networks (CNN) in the image fusion field. In this for encoding the maps , deep CNN networks are trained by higher quality image patches and their blurred versions. This technique greatly exhibits the potential of CNN for higher quality image fusion [238].

In a work presented by Jing Yang in 2017 an image fusion technique improving the spatial resolution of a hyperspectral (HS) image using non-local sparse representation in pixel grouping framework has been presented. This technique exploits the spectral non-local self-similarity and spectral sparsity of the (HS) image. A high spatial and spectral resolution hyper-spectral image is obtained by fusing the HS image and MS image with high spatial resolution. The proposed method is able to outperform several sparse representation based image fusion techniques [239].

In 2017 again a technique based on sparse representation and feature extraction is given to fuse multi-modal medical images (CT/MR, MR-T1/MR-T2, and CT/PET). This technique is designed using three decision maps which are structure information map (SM), energy information map (EM), structure and energy map (SEM). The method is able to achieve an improved overall quality of the fused image with the induction of high energy and structure information from source image to the fused image along with contrast enhancement [240].

In 2017 an image fusion technique based on IHS-wavelet transform domain has been proposed by Dogra *et al.* The cascaded method of image enhancement and image fusion for the fusion osseous and vascular is able to achieve an information transfer rate of 0.8513. This technique sets a trend for enhancing the source images prior to fusion of images [143].

VII. APPLICATIONS

In recent years pixel level image fusion has been employed in a wide variety of applications such as medical-diagnosis [50], remote-sensing [40], [241], photography applications [242]

and surveillance [136]. In this section some of the examples of the image fusion will be discussed.

A. MEDICAL IMAGE FUSION

There are various imaging modalities which are required to be fused for enhancing the visual perception in the medical diagnosis [243]. The enhanced fused image facilitates better visual perception to radiologists and further image processing tasks like CAD (computer aided diagnosis. The concept of image fusion has been extended to several clinical applications such as multi-modal and unimodal image fusion. For instance, for detection and removal of cerebral iron deposits T_1 weighted and T_2 weighted MRI (Magnetic Resonance Imaging) images are fused. For diagnosis related to lung cancer, PET (Positron Emission Tomography) and CT (Computed Tomography) are fused together . In medical diagnosis and studies related to abdomen, SPECT (Single Photon Emission Computed Tomography) and CT are fused together. CT and MRI images were fused for neuro- navigation in skull based tumor surgery. Ultrasound (sonography) MRI and image fusion has made study of vascular blood flow in various parts of the body very easy. The fusion of PET and MRI images has helped a lot in hepatic and metastasis detection and intracranial tumour diagnosis. SPECT and MRI images were fused together for the localization of abnormalities caused by tinnitus in patient body. Bone-vessel image fusion is another very significant field of application of image fusion in medical diagnosis. DSA is the principle radiographic technique aiding in the diagnosis of vascular diseases.

Following are the few examples of various applications of medical image fusion reported in literature. Fig. 8(c) shows the fusion of MRI (Fig. 8(a) and SPECT image (Fig. 8(b)) for the diagnosis of the Alzheimer's disease. These modalities have been fused using Optimum Spectrum Mask Fusion (OSMF) based on Grey Wolf optimizer algorithm. The optimum mask used in this scheme is able to capture higher number of salient features of the image. The fused image is able to deliver a greater amount of complimentary information relevant to clinical diagnosis. This method of image fusion given in [244] is also tested to fuse MRI-CT, MRI: T1-T2 and MRI-PET for the clinical diagnosis and treatment procedure of sarcoma, cerebral toxoplasmosis and astrocytoma (Fig. 8) [244].

The GWO is able to give better edge quality in the fused results using dynamic selection of scale values according to input data set [244].

The fusion of the DSA (Digital Subtraction Angiography) image and mask image provides the osseous and vascular information in a single image. This field of medical image fusion has become increasingly important for planning surgical procedures and thus abridging the time between the clinical diagnosis and treatment. DSA (Digital Subtraction Angiography) is an objectively recent technique which has been used for the diagnosis of the vascular diseases. DSA has a wide field of applications ranging from cerebrovascular

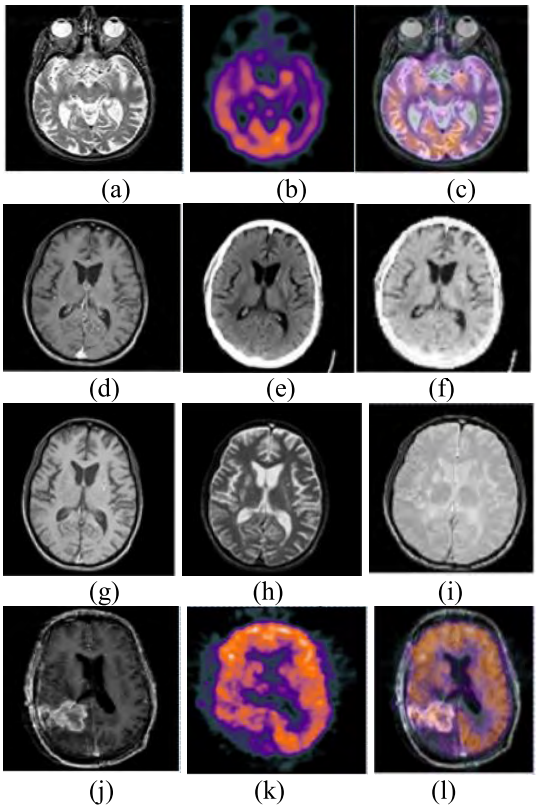

FIGURE 8. (a), (d), (g), (j)-MR image; (b) SPECT image; (e) CT image; (h) MRI-T2 image; (k) PET image; (c), (f), (i), (l) fused images [244].

diagnosis procedures to carotid artery studies [141], [142]. Dogra *et al.* [143] has proposed a transform and spatial domain based techniques to fuse the mask and the DSA images together. In this IHS-Wavelet transform based fusion technique has been employed to obtain a fusion of osseous and vascular image. The information transfer rate achieved in this method was as high as 0.8513.

This was achieved by pre-hand enhancement of the source images using Ripplet transform and Butterworth high pass filter. The innovative technique has shown to prove promising results for combining of bone and vessel information. On similar track the fusion of DSA and mask images has been depicted using Dense SIFT (Scale Invariant feature Transform) and Generalized Reisz Wavelet transform in [141] and [142] respectively. The fusion of the mask and DSA image proposed in [143] is depicted in Fig. 9 below.

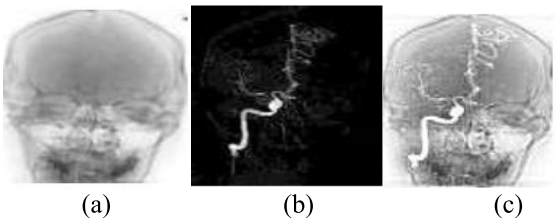

FIGURE 9. (a) Mask image; (b) DSA image; (c) fused image [143].

Shen *et al.* [6] presented the idea of volumetric image fusion PET and T1W MRI image using cross scale

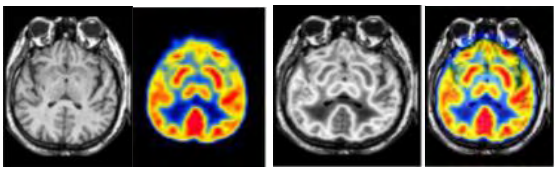

FIGURE 10. (a) PET image (color-coded); (b) T1W MRI image; (c) Fused image. (d) Fused image (luminance channel) [6].

fusion rule. This is illustrated in Fig. 8. This multi-scale decomposition based fusion method exploits both intrascale and interscale consistencies. By effective exploitation of the neighbourhood information an optimal set of coefficients is determined. The pixel information in the source image is blended in a monochrome format while preserving the contrast and the gradient information. The fusion algorithm results for MRI and PET image is also depicted in Figure10 using luminance channel. This technique for 3-D information fusion can be further exploited in 4-D domain.

An efficient fusion of mass spectrometric (MS) and microscopic images which is a multimodality paradigm for molecular tissue mapping is given in [245]. The IMS (imaging mass spectroscopy) generated by molecular mapping having coarse spatial resolution but rather rich in chemical information is fused with optical microscopy maps which have higher spatial resolution and are low on chemical specificity. The resulting fused images contain both a higher chemical specificity and higher spatial resolution. Multivariate regression is employed for modelling of the variable in one technology using variable from other technology. The IMS and MS image fusion is depicted in Fig. 11.

FIGURE 11. (a) IMS image; (b) MS image; (c) Fused image [245].

This was a brief review of various types of medical image fusion. Besides these above mentioned applications numerous researchers have presented several applications in context on medical image fusion. The major goal of the medical image fusion is the diagnosis and treatment of various clinical ailments and diseases. The large amount of literature on medical image fusion witnesses a huge amount of dependability of radiologists on image fusion techniques. However there are some issues like prevalence of noise and artefacts in the fused images due to the various imaging sensors and are still an open challenge for researchers.

B. REMOTE SENSING IMAGE FUSION

Remote sensing applications focus on extraction of required information about the surface of earth by acquiring images from a distant location. A remote sensing fusion algorithm aims at combining spatial, spectral and temporal variations in information of same or different scenes in a single image. Remote sensing systems observe the pixels of an image in the different sections of the electromagnetic spectrum such that these images vary in spatial, spectral and temporal resolution. These types of data sets include Multispectral images (MS) with high spectral resolution, lower spatial resolution and narrow spectral bandwidth, Panchromatic images (PAN) with wide spectral bandwidth and higher spatial resolution. The fusion of PAN images with MS images is called pan sharpening. The spectrum of PAN and MS images is closer to each other whereas the spectral distribution of hyperspectral images is quite large. This makes the fusion of PAN and MS images easier than the fusion of PAN and HS images. The fusion of these kinds of images combines the geometrical features of a scene in a single image such that the fused images provide more amount of conglomerated information than any of the individual images. Following are the few examples presented by various authors in the field of remote sensing.

In [247] proposed an adaptive IHS and multi-scale guided filter image fusion algorithm for the fusion of MS and PAN images. The method injected the detailed map extracted from the PAN images into MS images to sharpen its lower resolution. First the intensity components of the MS image are obtained and PAN images are filtered using multi-scale guided filter strategy. Then these decomposed coefficients are fused together using the proposed algorithm. Fig. 12 and 13 shows the fusion process of MS and PAN images for IKONOS and QUICKBIRD data set respectively. The method proposed in [247] has demonstrated to provide more spectral information and preserve higher spatial information than any of the individual remote sensing images.

FIGURE 12. IKONOS images: (a) MS image; (b) PAN image; (c) fused image [247].

In [214] another application based on fusion of remotely sensed multispectral and hyper-spectral images is reported. Fig. 14 shows the fusion of MS and HS images for AVIRIS data sets. To compensate for the spectral and the spatial blurring caused by sensor characteristics the high spectral resolution MS images and high spatial resolution (HS) images are fused in this paper. The article proposes a hierarchical Bayesian model to combine multiple numbers of multiband images with varying spatial and spectral resolution. A Markov chain Monte Carlo (MCMC) is formulated to

FIGURE 13. QUICKBIRD images: (a) MS image; (b) PAN image; (c) fused image [247].

FIGURE 14. AVIRIS images: (a) HS image (b) MS image (c) fused image [214].

obtain samples which have asymptotical distribution w.r.t. the target distribution to finally calculate the Bayesian estimate of the scene from its posterior distribution. The high dimensional distribution so obtained is efficiently sampled using Hamiltonian Monte Carlo step (HMC).

FIGURE 15. Pleiades images: (a) MS image (b) PAN image (c) fused image [248].

In Fig. 15 one other remote sensing application based on pan sharpening problem is shown. The figure depicts the fusion of PAN and MS images for Pleiades data set is fused for remote sensing application using morphological operator based algorithms reported in [248].

In the field of remote sensing spectral and spatial distortions are major challenging problem. The dissimilarities in the spatial and the spectral structures may introduce artefacts in the fusion process. Another major problem in remote sensing application is the mis-registration of the source images. Even the PAN and MS images which are captured at same platform are highly mis-registered because of the difference in the acquisition time and their orientation angles for image acquisition. In order to obtain an efficient solution of remote sensing problems these issues require prime attention.

C. MULTI-FOCUS IMAGE FUSION

Multi-focus image fusion is another branch of image fusion which aims at combining the focussed areas in the source images into a single image to make the fused image more suitable for human perception. Multi-focus image finds application in various fields, example for recognition of object and feature extraction in military surveillance as well as aeronautical observations. Several spatial and transform domain image fusion methods have been reported in literature for the fusion of multi-focus source images.

FIGURE 16. Desk data set: (a) Source image1 (b) source image 2 (c) fused image [249].

Fig. 16 summaries the problem of multi-focus image fusion of popular ''Desk'' data set reported in [249]. The source images with distinguished foci are combined by constructing gradient based decision maps and using mathematical morphology. In this method the weighted kernels based on image gradients are designed to roughly identify the focused regions. The morphological operations so performed adjusts the boundaries between the focused and defocused regions are true boundaries are hence extracted. The experiments based on this method reported to have obtained significant results in the field of multi-focus image fusion as compared to state-of-the-art.

In 2012, Kang et.al reported a compressed sensing framework for fusion of multi-focus images [250]. The proposed algorithm was tested for various data-sets. The results for clock data sets, reported in [250] are shown in Fig. 17.

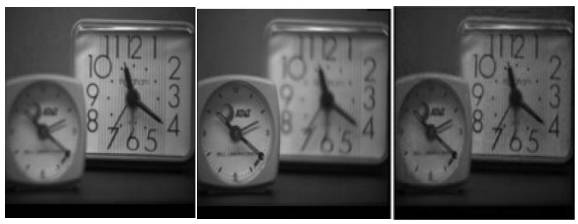

FIGURE 17. (a) Clock 1 (b) Clock 2 (c) Fused image [250].

The algorithm designed consists of three steps i.e. sampling of images, fusion measurement and image reconstruction. The dual channel PCNN is utilized for sampling of images and images are reconstructed using self-adaptively modified Landwebber filter. It can be seen from Fig. 17 that fused image efficiently brings both the clocks in focus.

The limited depth of focus of optical lens and lesser field depth make it impossible for optical cameras to produce a single image with all-in-focus. Therefore there arises a huge dependability on multi-focus image processing solutions.

FIGURE 18. (a) Visible image (b) infrared image (c) fused image [151].

There are a large number of image fusion methods reported in literature for fusion of multi-focus images. Besides military surveillance multi-focus image fusion finds its applications in meteorological phenomena and biomedical cell monitoring.

D. CONCEALED WEAPON DETECTION

Concealed weapon detection is an extremely interesting image fusion application. Concealed weapon detection is an important protocol in the area of law enforcement and terrorism. The low cost of thermal and infrared imaging sensors has enabled the detection of harmful weapons. The visible and infrared images are combined to detect and identify the concealed weapons. Fig. 18 shows a very popular example of concealed weapon detection reported in [151]. Fig. 18 (a) and (b) shows accurately aligned visible and infrared images. Due to the temperature difference between the body and the weapon metal, the weapon appears darker than the human body in the infrared image. However there is no sign of concealed weapon in the visible images. The two images are fused using colour fusion algorithm to provide the visibility of the concealed weapon in the coloured domain.

E. MULTI-EXPOSURE IMAGE FUSION

Ma *et al.* [256] proposed a simple yet robust structural patch decomposition based multi-exposure image fusion technique (SPD-MEF) to effectively overcome the ghosting artefacts in the fused images. The method has been applied on 21 static scenes and 19 dynamic scenes. Various experimental results given by authors demonstrate that the proposed method not only outperforms various state of the art multi-exposure fusion techniques on the static scenes but also produces high quality dynamic fused images with a very low amount of ghosting effects. One of the many results of the SPD-MEF approach on static scenes given in [256] is shown below.

The image patches from the source images are decomposed into three independent components e.g. signal strength, signal structure and mean intensity. The three components of each of the patches from the source images are fused separately and desired patch so obtained is placed back into the fused images. This patch based method gives lower computational overhead as it does not require post processing steps to improve visual quality. MEF forms a cost effective alternative to cover the gap between high dynamic range imaging and low dynamic range displays.

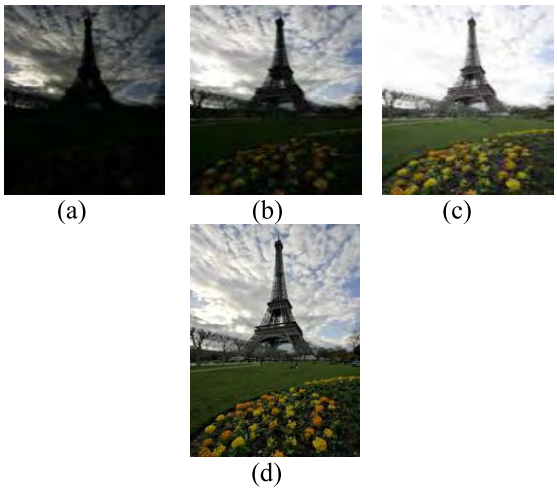

FIGURE 19. (a),(b),(c) Source images; (d) Fused image [256].

VIII. EXPERIMENTAL SETUP, RESULTS AND DISCUSSIONS

In this section various state-of-art fusion techniques are analysed in terms of quantitative evaluation. These methods are employed on Osseous and Vascular data sets acquired from PGIMER Chandigarh. The data set is 8-bit grey scale image with the spatial resolution of 256*256 pixels.

The selection of methods is based on the various state-of-the-art techniques which are representative of various classes of image fusion.

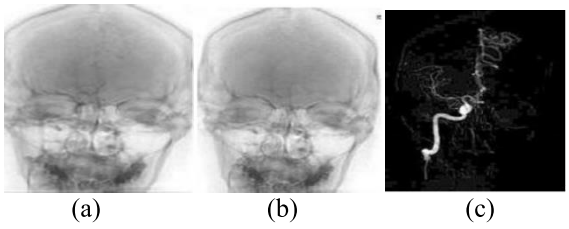

FIGURE 20. (a) contrast image (b) mask image (c) DSA image.

A. FUSION RESULT FOR OSSEOUS AND VASCULAR DATA

The source images taken for the quantitative analysis is shown in Fig. 20.

Fig. 20 (a) shows the contrast image which contains the vascular and osseous information, Fig. 20 (b) shows the mask image which contains the osseous information and Fig. 20 (c) shows the DSA image which contains the vascular information. DSA image is computed by subtracting the mask image from the contrast image. We have tested 10 state-of-the-art fusion techniques on our data set for comparative analysis.

The visual results for these techniques are shown in Fig. 21.

We have tested the performance of ten state-of-the-art image fusion techniques which are a) Laplacian pyramid [71], (b) ratio of low pass pyramid fusion [261], (c) wavelet fusion [260], (d) curvelet fusion [262], (e) multi resolution singular value decomposition [263], (f) guided filter

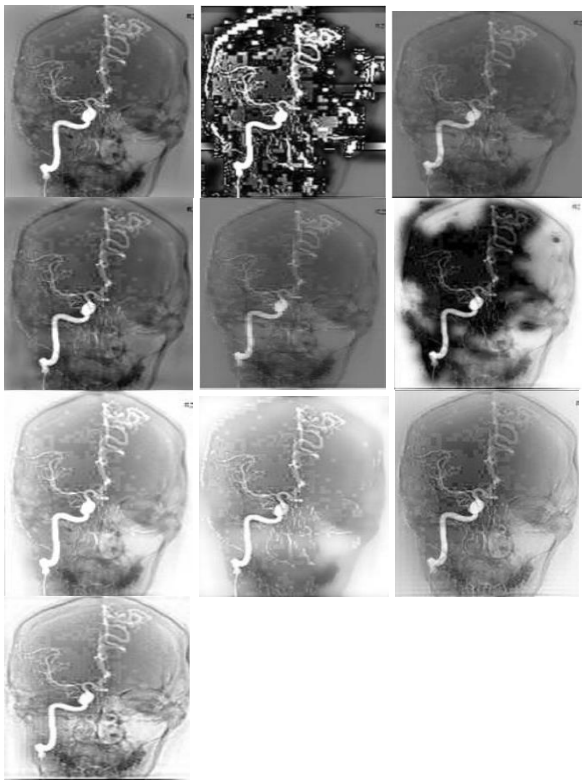

FIGURE 21. (a) Laplacian pyramid; (b) ratio of low pass pyramid fusion; (c) wavelet; [first row; left to right] (d) curvelet; (e) multi resolution singular value decomposition; (f) guided filter fusion; [second row; left to right] (g) Laplacian pyramid sparse representation (h) gradient transfer and total variation minimization; (i) osseous-vascular dense SIFT based fusion; [third row; left to right] (j) ripplet-IHS-wavelet based fusion.

fusion [135], (g) Laplacian pyramid sparse representation [207], (h) gradient transfer and total variation minimization [264], (i) osseous-vascular dense SIFT based fusion [141] (j) ripplet-IHS-wavelet based fusion [143]. The experiments are performed on a laptop with 3.3 Ghz Intel core CPU, 8GB and Matlab code.

In our experimental evaluation we focus on quantitative analysis of the various techniques in terms of osseous and vascular information. The results are analysed both subjectively and objectively. The results are analysed in terms of $Q^{AB/F}$ factor which gives the measurement of the transfer of a feature such as edges, textures and amount of information transferred from the source images to the fused composite image. It can be observed from table 3 that the highest value of information transfer rate is given by Laplacian pyramid based image fusion i.e. 0.9127. However there is an emergence of noise and artefacts in the fused image by this method which can be seen in Fig. 21(a). The second highest information fusion rate is achieved by Laplacian pyramid-sparse representation [LP-SR] based image fusion. Also the visual quality of the fused image obtained by this method is the highest. Besides these, the image enhancement based image fusion methods i.e. osseous-vascular dense SIFT based fusion and

TABLE 3. (a) Information transfer $Q^{RS/F}$ (b) Information loss $L^{RS/F}$.

Fusion rules	$Q^{RS/F}$	$L^{RS/F}$
(a)Laplacian pyramid [71, 143]	0.9127	0.0873
(b)ratio of low pass pyramid Fusion [263, 143]	0.4081	0.5919
(c)wavelet fusion [262]	0.7110	0.289
(d) Curvelet fusion [115]	0.8716	0.1284
(e)multi resolution singular value decomposition fusion [265,143]	0.6620	0.338
(f)guided filter fusion [135,143]	0.8140	0.186
(g) Laplacian pyramid sparse representation [207,143]	0.9115	0.0885
(h)gradient transfer-total variation minimization fusion[266,143]	0.6279	0.3721
(i)osseous-vascular dense SIFT based fusion[141]	0.7706	0.2294
(j)Ripplet-IHS-Wavelet based fusion [143]	0.8513	0.1487

ripplet-IHS-Wavelet based fusion method give comparable results as compared to LP-SR method. Also these methods are able to overcome the occurrence of noise and artefacts in the fused image. Another striking observation is the fusion by Guided filter. It can be seen though guided filter based image fusion gives acceptable information transfer rate, but the visual results are highly distorted. Most of the image fusion methods are based on the data sets which highly synchronised and possess high degree of similarity. Therefore the fusion of such kind of images is easily achievable. The osseous and vascular data sets are highly dissimilar to each other. Hence it becomes increasingly difficult to achieve an efficient fusion with proper alignment. This dissimilar attribute if the osseous and vascular data forms the basis for choosing them particularly for the analysis in this section. We have demonstrated the performance of various state-of –the art image fusion techniques on the fusion of DSA and mask images [143].

In the end it can be conclude that the medal of the state of the art image fusion techniques is held hybrid image enhancement based fusion techniques. The quality of the images to be fused directly affects the amount of transfer of gradient information from the source images to the composite fused image. Therefore as the quality of the source images, the information transfer rate also increases.

IX. CONCLUSION

The prime goal of image fusion is to generate a single fused which provides more reliable and accurate information than any one individual image and which gives higher amount of distinguishability amongst the features in the images. The technological advancements in the field of image fusion has made it very useful in medical diagnostics and monitoring, military and security surveillance, feature extraction and

object recognition. Researchers have been progressing very dynamically in devising advanced techniques. However each image fusion technique has its edges and limitations over the other. In this article a survey of various image fusion techniques at pixel has been conducted.

The image methods have been broadly classified into multi-scale decomposition based methods, non-multi-scale decomposition based methods, sparse representation based methods, PCA and IHS based methods and of course hybrid methods. It has been observed the main objectives of image fusion are as follows: to enhance the classification accuracy, to increase spatial resolution, to provide higher geometric precision and to enhance the perception for change detection or a defect.

From the literature survey it has been observed that inaccurate registration of the objects between the images or of the source images is strongly linked to poor performance of the image fusion techniques. Therefore proper registration and precise alignment of the source images is vital to ensure greater image fusion quality. Secondly it has been seen that a lot of stress has been laid on the improvement of the imaging quality and some regions of interest in the image. The requirement for improvisation the image quality arises from the existence of image noise and physical limitations of the image. Therefore removal of signal noise and enhancement of image feature details has shown to have a very positive impact on the image fusion process.

The selection of the image decomposition technique and the fusion rule are two basic steps of any kind of image fusion process. However it has been observed that the key role in image fusion is played by the image representation method rather than the fusion rule. As compared to the development of the decomposition methods, the fusion rules have not progressed much.

Furthermore it can be stated that fusion rules which consider higher correlation amongst the pixels can further improve the image fusion performance by eliminating defects like visual artefacts and noise. In context of the image representation methods most of the researchers focus on depicting the spatial structures of the images using different multi-scale decompositions such as pyramids, MGA tools and edge preserving filters. The major advantage of multi-scale decomposition methods is their ability to accurately segregate fine texture details at different scales but they fail drastically to represent low frequency components sparsely. The spatial domain methods are simple and easy to implement but these methods rely heavily on the precise estimation of the optimal weights for different pixels. Therefore to combine the advantages of both the methods novel hybrid fusion methods have reported. It has been found the novel sparse representation and convolutional representative methods have been the torch bearers in the field of image fusion. However the various image decomposition methods are sensitive to the similarity amongst the images. For instance cross bilateral fusion rule which has reported to give the highest fusion rate so far has failed drastically on fusion of dissimilar images. Besides in context of sparse representation and dictionary learning methods it is difficult to reconstruct the small-scale details of the source image with the limited number of atoms in the dictionary. Also these approaches are skewed towards the quality of the images selected for training data sets which can vary from one image to another. Therefore accurate fusion of highly dissimilar images is an open problem for the researchers.

Another challenging topic in image fusion is the fusion performance evaluation methods. It has been observed that recent evaluation metrics which do not require an ideal reference image (which is not always available) are more accurate in analysing the fusion performance. These are local feature based fusion metrics which provides the relative edge information travel information travel from input images to the fused images. However a very important question how to measure the complimentary information (spatial structures and global contrast) and visual artefacts appeared in the fused image. However since these gradient based methods are relative it can be stated that higher amount of information travel rate will lead to lesser amount of information loss and artefacts. Therefore researchers can focus on simultaneously on generalising fusion metrics for imperfect situations and on enhancement of source images prior to fusion to increase information transfer.

Besides this triple modality fusion is also a hot research topic for future researchers. The idea can be implemented opaque and semi-transparent source images.

In conclusion pixel level image fusion has progressed significantly in recent years which indicate the importance of this kind of research in various fields. Combining different methods and sparse representation methods are observed to be very successful in this field. However there stills exits numerous challenges in image fusion such as limitations of imaging hardware, computational complexities, image noise, objective evaluation metrics, dissimilarity between images, non-robust training data sets, resolution difference between images and imperfect environmental conditions. Therefore it is expected that innovative ideas and novel research contributions will keep surfacing and growing in the upcoming years.

REFERENCES

[1] Z. Zhang and R. S. Blum, "A categorization of multiscale-decomposition-based image fusion schemes with a performance study for a digital camera application," *Proc. IEEE*, vol. 87, no. 8, pp. 1315–1326, Aug. 1999.

[2] R. S. Blum and Z. Liu, Eds., *Multi-Sensor Image Fusion and Its Applications*. Boca Raton, FL, USA: CRC Press, 2005.

[3] D. L. Hall and J. Llinas, "An introduction to multisensor data fusion," *Proc. IEEE*, vol. 85, no. 1, pp. 6–23, Jan. 1997.

[4] Z. Wang, D. Ziou, C. Armenakis, D. Li, and Q. Li, "A comparative analysis of image fusion methods," *IEEE Trans. Geosci. Remote Sens.*, vol. 43, no. 6, pp. 1391–1402, Jun. 2005.

[5] H. Li, B. S. Manjunath, and S. K. Mitra, "Multi-sensor image fusion using the wavelet transform," in *Proc. IEEE Int. Conf. Image Process. (ICIP)*, vol. 1. Nov. 1994, pp. 51–55.

[6] R. Shen, I. Cheng, and A. Basu, "Cross-scale coefficient selection for volumetric medical image fusion," *IEEE Trans. Biomed. Eng.*, vol. 60, no. 4, pp. 1069–1079, Apr. 2013.

[7] S. Prabhakar and A. K. Jain, "Decision-level fusion in fingerprint verification," *Pattern Recognit.*, vol. 35, no. 4, pp. 861–874, 2002.

[8] A. A. Ross and R. Govindarajan, "Feature level fusion of hand and face biometrics," *Proc. SPIE*, vol. 5779, pp. 196–204, Apr. 2005.
[9] C. Pohl and J. L. Van Genderen, "Review article multisensor image fusion in remote sensing: Concepts, methods and applications," *Int. J. Remote Sens.*, vol. 19, no. 5, pp. 823–854, 1998.
[10] A. Toet and J. Walraven, "New false color mapping for image fusion," *Opt. Eng.*, vol. 35, no. 3, pp. 650–658, 1996.
[11] J. A. Patton, D. Delbeke, and M. P. Sandler, "Image fusion using an integrated, dual-head coincidence camera with X-ray tube-based attenuation maps," *J. Nucl. Med.*, vol. 41, no. 8, pp. 1364–1368, 2000.
[12] P. Gailloud, S. Oishi, and K. Murphy, "Three-dimensional fusion digital subtraction angiography: New reconstruction algorithm for simultaneous three-dimensional rendering of osseous and vascular information obtained during rotational angiography," *Amer. J. Neuroradiol.*, vol. 26, no. 4, pp. 908–911, 2005.
[13] S. Shimizu *et al.*, "A novel image fusion visualizes the angioarchitecture of the perforating arteries in the brain," *Amer. J. Neuroradiol.*, vol. 24, no. 10, pp. 2011–2014, 2003.
[14] W. R. Brody, "Digital subtraction angiography," *IEEE Trans. Nucl. Sci.*, vol. NS-29, no. 3, pp. 1176–1180, Jun. 1982.
[15] D. W. Townsend, T. Beyer, and T. M. Blodgett, "PET/CT scanners: A hardware approach to image fusion," *Seminars Nucl. Med.*, vol. 33, no. 3, pp. 193–204, 2003.
[16] M. S. Judenhofer *et al.*, "Simultaneous PET-MRI: A new approach for functional and morphological imaging," *Nature Med.*, vol. 14, no. 4, pp. 459–465, 2008.
[17] T. A. Wilson, S. K. Rogers, and M. Kabrisky, "Perceptual-based image fusion for hyperspectral data," *IEEE Trans. Geosci. Remote Sens.*, vol. 35, no. 4, pp. 1007–1017, Jul. 1997.
[18] S. Chaudhuri and K. Kotwal, *Hyperspectral Image Fusion*. New York, NY, USA: Springer, 2013.
[19] A. Dogra and M. S. Patterh, "CT and MRI brain images registration for clinical applications," *J. Cancer Sci. Therapy*, vol. 6, no. 1, pp. 18–26, 2014.
[20] M. Song, D. Tao, C. Chen, J. Bu, J. Luo, and C. Zhang, "Probabilistic exposure fusion," *IEEE Trans. Image Process.*, vol. 21, no. 1, pp. 341–357, Jan. 2012.
[21] C. Han, T. S. Hatsukami, and C. Yuan, "A multi-scale method for automatic correction of intensity non-uniformity in MR images," *J. Magn. Reson. Imag.*, vol. 13, no. 3, pp. 428–436, 2001.
[22] J. Portilla, V. Strela, M. J. Wainwright, and E. P. Simoncelli, "Adaptive Wiener denoising using a Gaussian scale mixture model in the wavelet domain," in *Proc. Int. Conf. Image Process.*, vol. 2. 2001, pp. 37–40.
[23] G. Piella, "A general framework for multiresolution image fusion: From pixels to regions," *Inf. Fusion*, vol. 4, no. 4, pp. 259–280, 2003.
[24] V. S. Petrovic and C. S. Xydeas, "Gradient-based multiresolution image fusion," *IEEE Trans. Image Process.*, vol. 13, no. 2, pp. 228–237, Feb. 2004.
[25] S. Chen, R. Zhang, H. Su, J. Tian, and J. Xia, "SAR and multispectral image fusion using generalized IHS transform based on à Trous wavelet and EMD decompositions," *IEEE Sensors J.*, vol. 10, no. 3, pp. 737–745, Mar. 2010.
[26] M. Gonzalez-Audicana, J. L. Saleta, R. G. Catalan, and R. Garcia, "Fusion of multispectral and panchromatic images using improved IHS and PCA mergers based on wavelet decomposition," *IEEE Trans. Geosci. Remote Sens.*, vol. 42, no. 6, pp. 1291–1299, Jun. 2004.
[27] Y. Zhang, "Understanding image fusion," *Photogramm. Eng. Remote Sens.*, vol. 70, no. 6, pp. 657–661, 2004.
[28] R. P. Desale and S. V. Verma, "Study and analysis of PCA, DCT & DWT based image fusion techniques," in *Proc. IEEE Int. Conf. Signal Process. Image Process. Pattern Recognit. (ICSIPR)*, Feb. 2013, pp. 66–69.
[29] M. Elad and M. Aharon, "Image denoising via sparse and redundant representations over learned dictionaries," *IEEE Trans. Image Process.*, vol. 15, no. 12, pp. 3736–3745, Dec. 2006.
[30] X. Otazu, M. González-Audícana, O. Fors, and J. Núñez, "Introduction of sensor spectral response into image fusion methods. Application to wavelet-based methods," *IEEE Trans. Geosci. Remote Sens.*, vol. 43, no. 10, pp. 2376–2385, Oct. 2005.
[31] A. Dogra, S. Agrawal, and B. Goyal, "Efficient representation of texture details in medical images by fusion of Ripplet and DDCT transformed images," *Tropical J. Pharmaceutical Res.*, vol. 15, no. 9, pp. 1983–1993, 2016.
[32] M. Choi, R. Y. Kim, M.-R. Nam, and H. O. Kim, "Fusion of multispectral and panchromatic Satellite images using the curvelet transform," *IEEE Geosci. Remote Sens. Lett.*, vol. 2, no. 2, pp. 136–140, Apr. 2005.
[33] W. Shi, C. Zhu, Y. Tian, and J. Nichol, "Wavelet-based image fusion and quality assessment," *Int. J. Appl. Earth Observat. Geoinf.*, vol. 6, nos. 3–4, pp. 241–251, 2005.
[34] K. Amolins, Y. Zhang, and P. Dare, "Wavelet based image fusion techniques—An introduction, review and comparison," *ISPRS J. Photogramm. Remote Sens.*, vol. 62, no. 4, pp. 249–263, 2007.
[35] G. Pajares and J. M. de la Cruz, "A wavelet-based image fusion tutorial," *Pattern Recognit.*, vol. 37, no. 9, pp. 1855–1872, 2004.
[36] S. G. Mallat, "A theory for multiresolution signal decomposition: The wavelet representation," *IEEE Trans. Pattern Anal. Mach. Intell.*, vol. 11, no. 7, pp. 674–693, Jul. 1989.
[37] M. Gonzàlez-Audícana, X. Otazu, O. Fors, and A. Seco, "Comparison between Mallat's and the 'à trous' discrete wavelet transform based algorithms for the fusion of multispectral and panchromatic images," *Int. J. Remote Sens.*, vol. 26, no. 3, pp. 595–614, 2005.
[38] H. Demirel and G. Anbarjafari, "Image resolution enhancement by using discrete and stationary wavelet decomposition," *IEEE Trans. Image Process.*, vol. 20, no. 5, pp. 1458–1460, May 2011.
[39] S. Li, J. T. Kwok, and Y. Wang, "Using the discrete wavelet frame transform to merge Landsat TM and SPOT panchromatic images," *Inf. Fusion*, vol. 3, no. 1, pp. 17–23, 2002.
[40] C. Thomas, T. Ranchin, L. Wald, and J. Chanussot, "Synthesis of multispectral images to high spatial resolution: A critical review of fusion methods based on remote sensing physics," *IEEE Trans. Geosci. Remote Sens.*, vol. 46, no. 5, pp. 1301–1312, May 2008.
[41] G. Vivone *et al.*, "A critical comparison among pansharpening algorithms," *IEEE Trans. Geosci. Remote Sens.*, vol. 53, no. 5, pp. 2565–2586, May 2015.
[42] S. Li, J. T. Kwok, and Y. Wang, "Multifocus image fusion using artificial neural networks," *Pattern Recognit. Lett.*, vol. 23, no. 8, pp. 985–997, 2002.
[43] G. Guorong, X. Luping, and F. Dongzhu, "Multi-focus image fusion based on non-subsampled shearlet transform," *IET Image Process.*, vol. 7, no. 6, pp. 633–639, 2013.
[44] M. Yin, W. Liu, X. Zhao, Y. Yin, and Y. Guo, "A novel image fusion algorithm based on nonsubsampled shearlet transform," *Optik-Int. J. Light Electron Opt.*, vol. 125, no. 10, pp. 2274–2282, 2014.
[45] S. Singh, D. Gupta, R. S. Anand, and V. Kumar, "Nonsubsampled shearlet based CT and MR medical image fusion using biologically inspired spiking neural network," *Biomed. Signal Process. Control*, vol. 18, pp. 91–101, Apr. 2015.
[46] G. Bhatnagar, Q. M. J. Wu, and Z. Liu, "Directive contrast based multimodal medical image fusion in NSCT domain," *IEEE Trans. Multimedia*, vol. 15, no. 5, pp. 1014–1024, Aug. 2013.
[47] Q. Zhang and B.-L. Guo, "Multifocus image fusion using the nonsubsampled contourlet transform," *Signal Process.*, vol. 89, no. 7, pp. 1334–1346, 2009.
[48] H. Ghassemian, "A review of remote sensing image fusion methods," *Inf. Fusion*, vol. 32, pp. 75–89, Nov. 2016.
[49] S. Li, X. Kang, L. Fang, J. Hu, and H. Yin, "Pixel-level image fusion: A survey of the state of the art," *Inf. Fusion*, vol. 33, pp. 100–112, Jan. 2017.
[50] A. P. James and B. V. Dasarathy, "Medical image fusion: A survey of the state of the art," *Inf. Fusion*, vol. 19, pp. 4–19, Sep. 2014.
[51] M. Kumar and S. Dass, "A total variation-based algorithm for pixel-level image fusion," *IEEE Trans. Image Process.*, vol. 18, no. 9, pp. 2137–2143, Sep. 2009.
[52] C. S. Xydeas and V. S. Petrovic, "Objective pixel-level image fusion performance measure," *Proc. SPIE*, vol. 4051, pp. 89–98, Apr. 2000.
[53] B. Yang, Z.-L. Jing, and H.-T. Zhao, "Review of pixel-level image fusion," *J. Shanghai Jiaotong Univ. (Sci.)*, vol. 15, no. 1, pp. 6–12, 2010.
[54] K. Rokni, A. Ahmad, K. Solaimani, and S. Hazini, "A new approach for surface water change detection: Integration of pixel level image fusion and image classification techniques," *Int. J. Appl. Earth Observat. Geoinf.*, vol. 34, pp. 226–234, Feb. 2015.
[55] M. Choi, "A new intensity-hue-saturation fusion approach to image fusion with a tradeoff parameter," *IEEE Trans. Geosci. Remote Sens.*, vol. 44, no. 6, pp. 1672–1682, Jun. 2006.

[56] P. S. Pradhan, R. L. King, N. H. Younan, and D. W. Holcomb, "Estimation of the number of decomposition levels for a wavelet-based multiresolution multisensor image fusion," *IEEE Trans. Geosci. Remote Sens.*, vol. 44, no. 12, pp. 3674–3686, Dec. 2006.

[57] L. Wald, "Some terms of reference in data fusion," *IEEE Trans. Geosci. Remote Sens.*, vol. 37, no. 3, pp. 1190–1193, May 1999.

[58] L. Shao, R. Yan, X. Li, and Y. Liu, "From heuristic optimization to dictionary learning: A review and comprehensive comparison of image denoising algorithms," *IEEE Trans. Cybern.*, vol. 44, no. 7, pp. 1001–1013, Jul. 2014.

[59] J. J. Lewis, R. J. O'Callaghan, S. G. Nikolov, D. R. Bull, and N. Canagarajah, "Pixel- and region-based image fusion with complex wavelets," *Inf. Fusion*, vol. 8, no. 2, pp. 119–130, 2007.

[60] K. Nandakumar, Y. Chen, S. C. Dass, and A. K. Jain, "Likelihood ratio-based biometric score fusion," *IEEE Trans. Pattern Anal. Mach. Intell.*, vol. 30, no. 2, pp. 342–347, Feb. 2008.

[61] M. Fauvel, J. Chanussot, and J. A. Benediktsson, "Decision fusion for the classification of urban remote sensing images," *IEEE Trans. Geosci. Remote Sens.*, vol. 44, no. 10, pp. 2828–2838, Oct. 2006.

[62] A. Meraoumia, S. Chitroub, and A. Bouridane, "Fusion of finger-knuckle-print and palmprint for an efficient multi-biometric system of person recognition," in *Proc. IEEE Int. Conf. Commun. (ICC)*, Jun. 2011, pp. 1–5.

[63] Z. Zhang, R. Wang, K. Pan, S. Z. Li, and P. Zhang, "Fusion of near infrared face and iris biometrics," in *Advances in Biometrics* (Lecture Notes in Computer Science), vol. 4642, S. W. Lee and S. Z. Li, Eds. Berlin, Germany: Springer, 2007, pp. 172–180.

[64] W. Dou, Y. Chen, X. Li, and D. Z. Sui, "A general framework for component substitution image fusion: An implementation using the fast image fusion method," *Comput. Geosci.*, vol. 33, no. 2, pp. 219–228, 2007.

[65] J. Choi, K. Yu, and Y. Kim, "A new adaptive component-substitution-based satellite image fusion by using partial replacement," *IEEE Trans. Geosci. Remote Sens.*, vol. 49, no. 1, pp. 295–309, Jan. 2011.

[66] B. Aiazzi, S. Baronti, and M. Selva, "Improving component substitution pansharpening through multivariate regression of MS+Pan data," *IEEE Trans. Geosci. Remote Sens.*, vol. 45, no. 10, pp. 3230–3239, Oct. 2007.

[67] M. M. Rahman, S. K. Antani, and G. R. Thoma, "A learning-based similarity fusion and filtering approach for biomedical image retrieval using SVM classification and relevance feedback," *IEEE Trans. Inf. Technol. Biomed.*, vol. 15, no. 4, pp. 640–646, Jul. 2011.

[68] Y.-F. Yao, X.-Y. Jing, and H.-S. Wong, "Face and palmprint feature level fusion for single sample biometrics recognition," *Neurocomputing*, vol. 70, nos. 7–9, pp. 1582–1586, 2007.

[69] M. B. A. Haghighat, A. Aghagolzadeh, and H. Seyedarabi, "Multi-focus image fusion for visual sensor networks in DCT domain," *Comput. Elect. Eng.*, vol. 37, no. 5, pp. 789–797, 2011.

[70] R. Redondo, F. Šroubek, S. Fischer, and G. Cristóbal, "Multifocus image fusion using the log-Gabor transform and a multisize windows technique," *Inf. Fusion*, vol. 10, no. 2, pp. 163–171, 2009.

[71] P. J. Burt and E. H. Adelson, "The Laplacian pyramid as a compact image code," *IEEE Trans. Commun.*, vol. C-31, no. 4, pp. 532–540, Apr. 1983.

[72] P. J. Burt and E. H. Adelson, "Merging images through pattern decomposition," *Proc. SPIE*, vol. 575, pp. 173–181, Dec. 1985.

[73] P. J. Burt, "A gradient pyramid basis for pattern-selective image fusion," in *Soc. Inf. Display Int. Symp. Dig. Tech. Papers*, 1992, pp. 467–470.

[74] A. Toet, "A morphological pyramidal image decomposition," *Pattern Recognit. Lett.*, vol. 9, no. 4, pp. 255–261, 1989.

[75] G. K. Matsopoulos, S. Marshall, and J. N. H. Brunt, "Multiresolution morphological fusion of MR and CT images of the human brain," *IEE Proc.-Vis., Image Signal Process.*, vol. 141, no. 3, pp. 137–142, Jun. 1994.

[76] Z. Liu, K. Tsukada, K. Hanasaki, Y. K. Ho, and Y. P. Dai, "Image fusion by using steerable pyramid," *Pattern Recognit. Lett.*, vol. 22, no. 9, pp. 929–939, 2001.

[77] A. Toet, L. J. van Ruyven, and J. M. Valeton, "Merging thermal and visual images by a contrast pyramid," *Opt. Eng.*, vol. 28, no. 7, p. 287789, 1989.

[78] P. J. Burt and R. J. Kolczynski, "Enhanced image capture through fusion," in *Proc. IEEE 4th Int. Conf. Comput. Vis.*, May 1993, pp. 173–182.

[79] S. Li, B. Yang, and J. Hu, "Performance comparison of different multi-resolution transforms for image fusion," *Inf. Fusion*, vol. 12, no. 2, pp. 74–84, Apr. 2011.

[80] Z. Xue, R. S. Blum, and Y. Li, "Fusion of visual and IR images for concealed weapon detection," in *Proc. IEEE 5th Int. Conf. Inf. Fusion*, vol. 2. Jul. 2002, pp. 1198–1205.

[81] S. Zheng, W.-Z. Shi, J. Liu, G.-X. Zhu, and J.-W. Tian, "Multisource image fusion method using support value transform," *IEEE Trans. Image Process.*, vol. 16, no. 7, pp. 1831–1839, Jul. 2007.

[82] J. J. Lewis, S. G. Nikolov, C. N. Canagarajah, D. R. Bull, and A. Toet, "Uni-modal versus joint segmentation for region-based image fusion," in *Proc. 9th Int. Conf. Inf. Fusion (ICIF)*, Florence, Italy, 2006, pp. 1–8, doi: 10.1109/ICIF.2006.301565.

[83] T. Chen, J. Zhang, and Y. Zhang, "Remote sensing image fusion based on ridgelet transform," in *Proc. IEEE Int. Geosci. Remote Sens. Symp. (IGARSS)*, vol. 2. Jul. 2005, pp. 1150–1153.

[84] F. E. Ali, I. M. El-Dokany, A. A. Saad, and F. E.-S. A. El-Samie, "Curvelet fusion of MR and CT images," *Prog. Electromagn. Res. C*, vol. 3, pp. 215–224, 2008.

[85] S. Li and B. Yang, "Multifocus image fusion by combining curvelet and wavelet transform," *Pattern Recognit. Lett.*, vol. 29, no. 9, pp. 1295–1301, 2008.

[86] M. Choi, R. Y. Kim, and M.-G. Kim, "The curvelet transform for image fusion," *Int. Soc. Photogramm. Remote Sens.*, vol. 35, pp. 59–64, Jul. 2004.

[87] J.-L. Starck, E. J. Candes, and D. L. Donoho, "The curvelet transform for image denoising," *IEEE Trans. Electron. Packag. Manuf.*, vol. 11, no. 6, pp. 670–684, Jun. 2002.

[88] E. Candès, L. Demanet, D. Donoho, and X. Ying, "Fast discrete curvelet transforms," *Multiscale Model. Simul.*, vol. 5, no. 3, pp. 861–899, Sep. 2006.

[89] E. J. Candes and D. L. Donoho, "Recovering edges in ill-posed inverse problems: Optimality of curvelet frames," *Ann. Statist.*, vol. 30, no. 3, pp. 784–842, 2002.

[90] E. J. Candes and D. L. Donoho, "Curvelets, multiresolution representation, and scaling laws," *Proc. SPIE*, vol. 4119, pp. 1–12, Dec. 2000.

[91] J. Xu, L. Yang, and D. Wu, "Ripplet: A new transform for image processing," *J. Vis. Commun. Image Represent.*, vol. 21, no. 7, pp. 627–639, 2010.

[92] S. Das and M. K. Kundu, "Ripplet based multimodality medical image fusion using pulse-coupled neural network and modified spatial frequency," in *Proc. IEEE Int. Conf. Recent Trends Inf. Syst. (ReTIS)*, Dec. 2011, pp. 229–234.

[93] M. Ghahremani and H. Ghassemian, "Remote sensing image fusion using ripplet transform and compressed sensing," *IEEE Geosci. Remote Sens. Lett.*, vol. 12, no. 3, pp. 502–506, Mar. 2015.

[94] A. Dogra and S. Agrawal, "Efficient image representation based on ripplet transform and pure-let," *Int. J. Pharm. Sci. Rev. Res.*, vol. 34, no. 2, pp. 93–97, 2015.

[95] A. Dogra and S. Agrawal, "3-Stage enhancement of medical images using ripplet transform, high pass filters and histogram equalization techniques," *Int. J. Pharmacy Technol.*, vol. 7, pp. 9748–9763, Dec. 2015.

[96] X.-B. Qu, J.-W. Yan, H.-Z. Xiao, and Z.-Q. Zhu, "Image fusion algorithm based on spatial frequency-motivated pulse coupled neural networks in nonsubsampled contourlet transform domain," *Acta Autom. Sinica*, vol. 34, no. 12, pp. 1508–1514, 2008.

[97] P. Ganasala and V. Kumar, "CT and MR image fusion scheme in non-subsampled contourlet transform domain," *J. Digit. Imag.*, vol. 27, no. 3, pp. 407–418, 2014.

[98] M. Qiguang and W. Baoshu, "A novel image fusion method using contourlet transform," in *Proc. IEEE Int. Conf. Commun., Circuits Syst.*, vol. 1. Jun. 2006, pp. 548–552.

[99] S. Yang, M. Wang, L. Jiao, R. Wu, and Z. Wang, "Image fusion based on a new contourlet packet," *Inf. Fusion*, vol. 11, no. 2, pp. 78–84, 2010.

[100] G. Easley, D. Labate, and W.-Q. Lim, "Sparse directional image representations using the discrete shearlet transform," *Appl. Comput. Harmon. Anal.*, vol. 25, no. 1, pp. 25–46, Jul. 2008.

[101] W.-Q. Lim, "The discrete shearlet transform: A new directional transform and compactly supported shearlet frames," *IEEE Trans. Image Process.*, vol. 19, no. 5, pp. 1166–1180, May 2010.

[102] S. Yi, D. Labate, G. R. Easley, and H. Krim, "A shearlet approach to edge analysis and detection," *IEEE Trans. Image Process.*, vol. 18, no. 5, pp. 929–941, May 2009.

[103] W. Kong and J. Liu, "Technique for image fusion based on nonsubsampled shearlet transform and improved pulse-coupled neural network," *Opt. Eng.*, vol. 52, no. 1, p. 017001, 2013.

[104] Y.-C. Lin, Q.-H. Liu, L. Tao, L. Song, and M.-R. Zhao, "An image fusion algorithm based on Directionlet transform," *Nanotechnol. Precis. Eng.*, vol. 8, no. 6, pp. 565–568, 2010.

[105] J. Teng, X. Wang, J. Zhang, S. Wang, and P. Huo, "A multimodality medical image fusion algorithm based on wavelet transform," in *Advances in Swarm Intelligence* (Lecture Notes in Computer Science). vol. 6146, Y. Tan, Y. Shi, and K. C. Tan, Eds. Berlin, Germany: Springer-Verlag, 2010, pp. 627–633.

[106] M. Agrawal, P. Tsakalides, and A. Achim, "Medical image fusion using the convolution of meridian distributions," in *Proc. Annu. Int. Conf. IEEE Eng. Med. Biol. Soc. (EMBC)*, Aug./Sep. 2010, pp. 3727–3730.

[107] B. V. Dasarathy, "Information fusion in the realm of medical applications—A bibliographic glimpse at its growing appeal," *Inf. Fusion*, vol. 13, no. 1, pp. 1–9, 2012.

[108] L. Chiorean and M.-F. Vaida, "Medical image fusion based on discrete wavelet transform using Java technology," in *Proc. IEEE ITI 31st Int. Conf. Inf. Technol. Interfaces (ITI)*, Jun. 2009, pp. 55–60.

[109] L. Yang, B. L. Guo, and W. Ni, "Multimodality medical image fusion based on multiscale geometric analysis of contourlet transform," *Neurocomputing*, vol. 72, nos. 1–3, pp. 203–211, 2008.

[110] B. Yang and Z. Jing, "Medical image fusion with a shift-invariant morphological wavelet," in *Proc. IEEE Conf. Cybern. Intell. Syst.*, Sep. 2008, pp. 175–178.

[111] Z. Wencang and C. Lin, "Medical image fusion method based on wavelet multi-resolution and entropy," in *Proc. IEEE Int. Conf. Autom. Logistics (ICAL)*, Sep. 2008, pp. 2329–2333.

[112] S. Cheng, J. He, and Z. Lv, "Medical image of PET/CT weighted fusion based on wavelet transform," in *Proc. IEEE 2nd Int. Conf. Bioinformatics Biomed. Eng. (ICBBE)*, May 2008, pp. 2523–2525.

[113] A. Wang, H. Sun, and Y. Guan, "The application of wavelet transform to multi-modality medical image fusion," in *Proc. IEEE Int. Conf. Netw., Sens. Control (ICNSC)*, Apr. 2006, pp. 270–274.

[114] K. Harish and D. Singh, "Quality assessment of fused image of MODIS and PALSAR," *Prog. Electromagn. Res. B*, vol. 24, pp. 191–221, 2010.

[115] F. Nencini, A. Garzelli, S. Baronti, and L. Alparone, "Remote sensing image fusion using the curvelet transform," *Inf. Fusion*, vol. 8, no. 2, pp. 143–156, 2007.

[116] M. N. Do and M. Vetterli, "The contourlet transform: An efficient directional multiresolution image representation," *IEEE Trans. Image Process.*, vol. 14, no. 12, pp. 2091–2106, Dec. 2005.

[117] K. P. Upla, M. V. Joshi, and P. P. Gajjar, "An edge preserving multiresolution fusion: Use of contourlet transform and MRF prior," *IEEE Trans. Geosci. Remote Sens.*, vol. 53, no. 6, pp. 3210–3220, Jun. 2015.

[118] S. Das, M. Chowdhury, and M. K. Kundu, "Medical image fusion based on ripplet transform type-I," *Prog. Electromagn. Res. B*, vol. 30, pp. 355–370, 2011.

[119] E. Angelini, Y. J. P. Esser, R. Van Heertum, and A. Laine, "Fusion of brushlet and wavelet denoising methods for nuclear images," in *Proc. IEEE Int. Symp. Biomed. Imag., Nano Macro*, Apr. 2004, pp. 1187–1191.

[120] F. Liu, J. Liu, and Y. Gao, "Image fusion based on wedgelet and wavelet," in *Proc. IEEE Int. Symp. Intell. Signal Process. Commun. Syst. (ISPACS)*, Nov./Dec. 2007, pp. 682–685.

[121] X. Yan, H.-L. Qin, S.-Q. Liu, T.-W. Yang, Z.-J. Yang, and L.-Z. Xue, "Image fusion based on tetrolet transform," *J. Optoelectron. Laser*, vol. 24, no. 8, pp. 1629–1633, 2013.

[122] F. A. Alomar, G. Muhammad, H. Aboalsamh, M. Hussain, A. M. Mirza, and G. Bebis, "Gender recognition from faces using bandlet and local binary patterns," in *Proc. IEEE 20th Int. Conf. Syst., Signals Image Process. (IWSSIP)*, Jul. 2013, pp. 59–62.

[123] G. R. Easley, D. Labate, and F. Colonna, "Shearlet-based total variation diffusion for denoising," *IEEE Trans. Image Process.*, vol. 18, no. 2, pp. 260–268, Feb. 2009.

[124] Y. Cao, S. Li, and J. Hu, "Multi-focus image fusion by nonsubsampled shearlet transform," in *Proc. IEEE 6th Int. Conf. Image Graph. (ICIG)*, Aug. 2011, pp. 17–21.

[125] L. Zhang and X. Wu, "An edge-guided image interpolation algorithm via directional filtering and data fusion," *IEEE Trans. Image Process.*, vol. 15, no. 8, pp. 2226–2238, Aug. 2006.

[126] J. G. Liu, "Smoothing filter-based intensity modulation: A spectral preserve image fusion technique for improving spatial details," *Int. J. Remote Sens.*, vol. 21, no. 18, pp. 3461–3472, 2000.

[127] F. Durand and J. Dorsey, "Fast bilateral filtering for the display of high-dynamic-range images," *ACM Trans. Graph.*, vol. 21, no. 3, pp. 257–266, 2002.

[128] A. Dogra, S. Agrawal, N. Khandelwal, and C. Ahuja, "Osseous and vascular information fusion using various spatial domain filters," *Res. J. Pharmacy Technol.*, vol. 9, no. 7, pp. 937–941, 2016.

[129] B. K. S. Kumar, "Image fusion based on pixel significance using cross bilateral filter," *Signal, Image Video Process.*, vol. 9, no. 5, pp. 1193–1204, 2015.

[130] J. Yadav, A. Dogra, B. Goyal, and S. Agrawal, "A review on image fusion methodologies and applications," *Res. J. Pharmacy Technol.*, vol. 10, no. 4, pp. 1239–1251, 2017.

[131] K. N. Chaudhury and K. Rithwik, "Image denoising using optimally weighted bilateral filters: A SURE and fast approach," in *Proc. IEEE Int. Conf. Image Process. (ICIP)*, Sep. 2015, pp. 108–112.

[132] M. Elad, "On the origin of the bilateral filter and ways to improve it," *IEEE Trans. Image Process.*, vol. 11, no. 10, pp. 1141–1151, Oct. 2002.

[133] Q. Zhang, X. Shen, L. Xu, and J. Jia, "Rolling guidance filter," in *Proc. Eur. Conf. Comput. Vis.*, 2014, pp. 815–830.

[134] J. Hu and S. Li, "The multiscale directional bilateral filter and its application to multisensor image fusion," *Inf. Fusion*, vol. 13, no. 3, pp. 196–206, 2012.

[135] S. Li, X. Kang, and J. Hu, "Image fusion with guided filtering," *IEEE Trans. Image Process.*, vol. 22, no. 7, pp. 2864–2875, Jul. 2013.

[136] Z. Zhou, B. Wang, S. Li, and M. Dong, "Perceptual fusion of infrared and visible images through a hybrid multi-scale decomposition with Gaussian and bilateral filters," *Inf. Fusion*, vol. 30, pp. 15–26, Jul. 2016.

[137] U. G. Gangkofner, P. S. Pradhan, and D. W. Holcomb, "Optimizing the high-pass filter addition technique for image fusion," *Photogramm. Eng. Remote Sens.*, vol. 74, no. 9, pp. 1107–1118, 2008.

[138] O. Rockinger and T. Fechner, "Pixel-level image fusion: The case of image sequences," *Proc. SPIE*, vol. 3374, pp. 378–388, Jul. 1998.

[139] E. Lallier and M. Farooq, "A real time pixel-level based image fusion via adaptive weight averaging," in *Proc. IEEE 3rd Int. Conf. Inf. Fusion (FUSION)*, vol. 2. Jul. 2000, p. WEC3-3.

[140] C. W. Therrien, J. W. Scrofani, and W. K. Kreb, "An adaptive technique for the enhanced fusion of low-light visible with uncooled thermal infrared imagery," in *Proc. IEEE Int. Conf. Image Process.*, vol. 1. Oct. 1997, pp. 405–408.

[141] A. Dogra, S. Agrawal, B. Goyal, N. Khandelwal, and C. K. Ahuja, "Color and grey scale fusion of osseous and vascular information," *J. Comput. Sci.*, vol. 17, pp. 103–114, Nov. 2016.

[142] A. Dogra, B. Goyal, and S. Agrawal, "Bone vessel image fusion via generalized reisz wavelet transform using averaging fusion rule," *J. Comput. Sci.*, to be published.

[143] A. Dogra, B. Goyal, S. Agrawal, and C. K. Ahuja, "Efficient fusion of osseous and vascular details in wavelet domain," *Pattern Recognit. Lett.*, vol. 94, pp. 189–193, Jul. 2017.

[144] J. J. Clark and A. L. Yuille, *Data Fusion for Sensory Information Processing Systems*, vol. 10. Boston, MA, USA: Kluwer, 1990, pp. 1–3.

[145] R. S. Blum and J. Yang, *Image Fusion Using the Expectation-Maximization Algorithm and a Gaussian Mixture Model*. Norwell, MA, USA: Kluwer, 2003.

[146] R. Shen, I. Cheng, and A. Basu, "QoE-based multi-exposure fusion in hierarchical multivariate Gaussian CRF," *IEEE Trans. Image Process.*, vol. 22, no. 6, pp. 2469–2478, Jun. 2013.

[147] W. A. Wright, "Quick Markov random field image fusion," *Proc. SPIE*, vol. 3374, pp. 302–308, Jul. 1998.

[148] R. Azencott, B. Chalmond, and F. Coldefy, "Markov fusion of a pair of noisy images to detect intensity valleys," *Int. J. Comput. Vis.*, vol. 16, no. 2, pp. 135–145, 1995.

[149] M. Aguilar and J. R. New, "Fusion of multi-modality volumetric medical imagery," in *Proc. IEEE 5th Int. Conf. Inf. Fusion*, vol. 2. Jul. 2002, pp. 1206–1212.

[150] A. M. Waxman, M. Aguilar, R. A. Baxter, D. A. Fay, and D. B. Ireland, "Opponent-color fusion of multi-sensor imagery: Visible, IR and SAR," Massachusetts Inst. Technol., Lincoln Lab, Lexington, MA, USA, Tech. Rep. 0704-0188, 1998.

[151] Z. Xue and R. S. Blum, "Concealed weapon detection using color image fusion," in *Proc. 6th Int. Conf. Inf. Fusion*, vol. 1. 2003, pp. 622–627.

[152] W. Huang and Z. Jing, "Multi-focus image fusion using pulse coupled neural network," *Pattern Recognit. Lett.*, vol. 28, no. 9, pp. 1123–1132, 2007.

[153] Z. Wang, Y. Ma, F. Cheng, and L. Yang, "Review of pulse-coupled neural networks," *Image Vis. Comput.*, vol. 28, no. 1, pp. 5–13, 2010.

[154] T. Lindblad and J. M. Kinser, *Image Processing Using Pulse-Coupled Neural Networks*. Berlin, Germany: Springer, 1998.

[155] S. Mitra and S. K. Pal, "Fuzzy multi-layer perceptron, inferencing and rule generation," *IEEE Trans. Neural Netw.*, vol. 6, no. 1, pp. 51–63, Jan. 1995.

[156] D. Ciregan, U. Meier, and J. Schmidhuber, "Multi-column deep neural networks for image classification," in *Proc. IEEE Conf. Comput. Vis. Pattern Recognit. (CVPR)*, Jun. 2012, pp. 3642–3649.

[157] J. L. Johnson, M. P. Schamschula, R. Inguva, and H. J. Caulfield, "Pulse-coupled neural network sensor fusion," *Proc. SPIE*, vol. 3376, pp. 219–226, Mar. 1998.

[158] R. P. Broussard, S. K. Rogers, M. E. Oxley, and G. L. Tarr, "Physiologically motivated image fusion for object detection using a pulse coupled neural network," *IEEE Trans. Neural Netw.*, vol. 10, no. 3, pp. 554–563, May 1999.

[159] Q. P. Zhang, W. J. Tang, L. L. Lai, W. C. Sun, and K. P. Wong, "Medical diagnostic image data fusion based on wavelet transformation and self-organising features mapping neural networks," in *Proc. IEEE Int. Conf. Mach. Learn.*, vol. 5. Aug. 2004, pp. 2708–2712.

[160] H. Szu *et al.*, "Early tumor detection by multiple infrared unsupervised neural nets fusion," in *Proc. 25th Annu. Int. Conf. IEEE Eng. Med. Biol. Soc.*, vol. 2. Sep. 2003, pp. 1133–1136.

[161] Y.-P. Wang, J.-W. Dang, Q. Li, and S. Li, "Multimodal medical image fusion using fuzzy radial basis function neural networks," in *Proc. Int. Conf. IEEE Wavelet Anal. Pattern Recognit. (ICWAPR)*, vol. 2. Nov. 2007, pp. 778–782.

[162] F. Masulli and S. Mitra, "Natural computing methods in bioinformatics: A survey," *Inf. Fusion*, vol. 10, no. 3, pp. 211–216, 2009.

[163] Y. Zhang, L. Chen, Z. Zhao, J. Jia, and J. Liu, "Multi-focus image fusion based on robust principal component analysis and pulse-coupled neural network," *Optik-Int. J. Light Electron Opt.*, vol. 125, no. 17, pp. 5002–5006, 2014.

[164] Z. Wang and Y. Ma, "Medical image fusion using *m*-PCNN," *Inf. Fusion*, vol. 9, no. 2, pp. 176–185, 2008.

[165] R. Wasserman, R. Acharya, C. Sibata, and K. H. Shin, "A data fusion approach to tumor delineation," in *Proc. IEEE Int. Conf. Image Process.*, vol. 2. Oct. 1995, pp. 476–479.

[166] G. N. Brock, W. D. Beavis, and L. S. Kubatko, "Fuzzy logic and related methods as a screening tool for detecting gene regulatory networks," *Inf. Fusion*, vol. 10, no. 3, pp. 250–259, 2009.

[167] M. Bhattacharya and A. Das, "Multimodality medical image registration and fusion techniques using mutual information and genetic algorithm-based approaches," in *Software Tools and Algorithms for Biological Systems*. New York, NY, USA: Springer, 2011, pp. 441–449.

[168] I. Bloch, O. Colliot, O. Camara, and T. Géraud, "Fusion of spatial relationships for guiding recognition, example of brain structure recognition in 3D MRI," *Pattern Recognit. Lett.*, vol. 26, no. 4, pp. 449–457, 2005.

[169] A. Villéger, L. Ouchchane, J.-J. Lemaire, and J.-Y. Boire, "Data fusion and fuzzy spatial relationships for locating deep brain stimulation targets in magnetic resonance images," in *Advanced Concepts for Intelligent Vision Systems*. Berlin, Germany: Springer, 2006, pp. 909–919.

[170] X. Tai and W. Song, "An improved approach based on FCM using feature fusion for medical image retrieval," in *Proc. IEEE 4th Int. Conf. Fuzzy Syst. Knowl. Discovery (FSKD)*, vol. 2. Aug. 2007, pp. 336–342.

[171] W. Song and T. Hua, "Analytic implementation for medical image retrieval based on FCM using feature fusion with relevance feedback," in *Proc. 2nd Int. Conf. Bioinform. Biomed. Eng. (ICBBE)*, May 2008, pp. 2590–2595.

[172] A Das and M Bhattacharya, "Evolutionary algorithm based automated medical image fusion technique: Comparative study with fuzzy fusion approach," in *Proc. World Congr. Nature Biol. Inspired Comput. (NaBIC)*, Dec. 2009, pp. 269–274.

[173] T. M. Chung, X. H. Liu, C. H. Chen, X. N. Sun, N. T. Chiu, and J. X. Lee, "Intermodality registration and fusion of liver images for medical diagnosis," in *Proc. Intell. Inf. Syst. (IIS)*, 2002, pp. 42–46.

[174] J. K. Avor and T. Sarkodie-Gyan, "An approach to sensor fusion in medical robots," in *Proc. IEEE Int. Conf. Rehabil. Robot. (ICORR)*, 2009, pp. 818–822.

[175] H.-J. Zimmermann, *Fuzzy Set Theory—And Its Applications*. The Netherlands: Springer, 2011.

[176] C. T. Kavitha and C. Chellamuthu, "Multimodal medical image fusion based on integer wavelet transform and neuro-fuzzy," in *Proc. Int. Conf. Signal Image Process. (ICSIP)*, 2010, pp. 296–300.

[177] B. Yang and S. Li, "Multifocus image fusion and restoration with sparse representation," *IEEE Trans. Instrum. Meas.*, vol. 59, no. 4, pp. 884–892, Apr. 2010.

[178] Y. C. Pati, R. Rezaiifar, and P. S. Krishnaprasad, "Orthogonal matching pursuit: Recursive function approximation with applications to wavelet decomposition," in *Proc. Conf. Rec. 27th Asilomar Conf. Signals, Syst. Comput.*, 1993, pp. 40–44.

[179] S. Li, H. Yin, and L. Fang, "Group-sparse representation with dictionary learning for medical image denoising and fusion," *IEEE Trans. Biomed. Eng.*, vol. 59, no. 12, pp. 3450–3459, Dec. 2012.

[180] B. Yang and S. Li, "Pixel-level image fusion with simultaneous orthogonal matching pursuit," *Inf. Fusion*, vol. 13, no. 1, pp. 10–19, 2012.

[181] H. Yin and S. Li, "Multimodal image fusion with joint sparsity model," *Opt. Eng.*, vol. 50, no. 6, p. 067007, 2011.

[182] N. Yu, T. Qiu, F. Bi, and A. Wang, "Image features extraction and fusion based on joint sparse representation," *IEEE J. Sel. Topics Signal Process.*, vol. 5, no. 5, pp. 1074–1082, Sep. 2011.

[183] Q. Zhang, Y. Fu, H. Li, and J. Zou, "Dictionary learning method for joint sparse representation-based image fusion," *Opt. Eng.*, vol. 52, no. 5, p. 057006, 2013.

[184] S. Li, H. Yin, and L. Fang, "Remote sensing image fusion via sparse representations over learned dictionaries," *IEEE Trans. Geosci. Remote Sens.*, vol. 51, no. 9, pp. 4779–4789, Sep. 2013.

[185] X. X. Zhuc and R. Bamler, "A sparse image fusion algorithm with application to pan-sharpening," *IEEE Trans. Geosci. Remote Sens.*, vol. 51, no. 5, pp. 2827–2836, May 2013.

[186] R. Rubinstein, A. M. Bruckstein, and M. Elad, "Dictionaries for sparse representation modeling," *Proc. IEEE*, vol. 98, no. 6, pp. 1045–1057, Jun. 2010.

[187] M. Kim, D. K. Han, and H. Ko, "Joint patch clustering-based dictionary learning for multimodal image fusion," *Inf. Fusion*, vol. 27, pp. 198–214, Jan. 2016.

[188] W. Wang, L. Jiao, and S. Yang, "Fusion of multispectral and panchromatic images via sparse representation and local autoregressive model," *Inf. Fusion*, vol. 20, pp. 73–87, Nov. 2014.

[189] T.-M. Tu, S.-C. Su, H.-C. Shyu, and P. S. Huang, "A new look at IHS-like image fusion methods," *Inf. Fusion*, vol. 2, no. 3, pp. 177–186, 2001.

[190] T.-M. Tu, P. S. Huang, C.-L. Hung, and C.-P. Chang, "A fast intensity-hue-saturation fusion technique with spectral adjustment for IKONOS imagery," *IEEE Geosci. Remote Sens. Lett.*, vol. 1, no. 4, pp. 309–312, Oct. 2004.

[191] N. Mitianoudis and T. Stathaki, "Pixel-based and region-based image fusion schemes using ICA bases," *Inf. Fusion*, vol. 8, no. 2, pp. 131–142, 2007.

[192] H. R. Shahdoosti and H. Ghassemian, "Combining the spectral PCA and spatial PCA fusion methods by an optimal filter," *Inf. Fusion*, vol. 27, pp. 150–160, Jan. 2016.

[193] C. A. Laben and B. V. Brower, "Process for enhancing the spatial resolution of multispectral imagery using pan-sharpening," U.S. Patent 6 011 875 A, Jan. 4, 2000.

[194] Y. Jiang and M. Wang, "Image fusion with morphological component analysis," *Inf. Fusion*, vol. 18, pp. 107–118, Jul. 2014.

[195] S. Li, J. T. Kwok, and Y. Wang, "Combination of images with diverse focuses using the spatial frequency," *Inf. Fusion*, vol. 2, no. 3, pp. 169–176, 2001.

[196] I. De and B. Chanda, "Multi-focus image fusion using a morphology-based focus measure in a quad-tree structure," *Inf. Fusion*, vol. 14, no. 2, pp. 136–146, 2013.

[197] X. Bai, Y. Zhang, F. Zhou, and B. Xue, "Quadtree-based multi-focus image fusion using a weighted focus-measure," *Inf. Fusion*, vol. 22, pp. 105–118, Mar. 2015.

[198] X. Zhang, H. Lin, X. Kang, and S. Li, "Multi-modal image fusion with KNN matting," in *Proc. Chin. Conf. Pattern Recognit.*, 2014, pp. 89–96.

[199] F. Chen, F. Qin, G. Peng, and S. Chen, "Fusion of remote sensing images using improved ICA mergers based on wavelet decomposition," *Proc. Eng.*, vol. 29, pp. 2938–2943, Jan. 2012.

[200] M. Ghahremani and H. Ghassemian, "A compressed-sensing-based pan-sharpening method for spectral distortion reduction," *IEEE Trans. Geosci. Remote Sens.*, vol. 54, no. 4, pp. 2194–2206, Apr. 2016.

[201] S. A. Valizadeh and H. Ghassemian, "Remote sensing image fusion using combining IHS and Curvelet transform," in *Proc. Sixth Int. Symp. Telecommun. (IST)*, Nov. 2012, pp. 1184–1189.

[202] C. He, Q. Liu, H. Li, and H. Wang, "Multimodal medical image fusion based on IHS and PCA," *Proc. Eng.*, vol. 7, pp. 280–285, Jan. 2010.

[203] J. Nunez, X. Otazu, O. Fors, A. Prades, V. Pala, and R. Arbiol, "Multiresolution-based image fusion with additive wavelet decomposition," *IEEE Trans. Geosci. Remote Sens.*, vol. 37, no. 3, pp. 1204–1211, May 1999.

[204] B. Huang, H. Song, H. Cui, J. Peng, and Z. Xu, "Spatial and spectral image fusion using sparse matrix factorization," *IEEE Trans. Geosci. Remote Sens.*, vol. 52, no. 3, pp. 1693–1704, Mar. 2014.

[205] Y. Luo, R. Liu, and Y. F. Zhu, "Fusion of remote sensing image base on the PCA+ ATROUS wavelet transform," *Int. Arch. Photogram., Remote Sens. Spatial Inf. Sci.*, vol. 37, pp. 1155–1158, Jun. 2008.

[206] S. Li and B. Yang, "Hybrid multiresolution method for multisensor multimodal image fusion," *IEEE Sensors J.*, vol. 10, no. 9, pp. 1519–1526, Sep. 2010.

[207] Y. Liu, S. Liu, and Z. Wang, "A general framework for image fusion based on multi-scale transform and sparse representation," *Inf. Fusion*, vol. 24, pp. 147–164, Jul. 2015.

[208] S. Li, J. T. Y. Kwok, I. W. H. Tsang, and Y. Wang, "Fusing images with different focuses using support vector machines," *IEEE Trans. Neural Netw.*, vol. 15, no. 6, pp. 1555–1561, Nov. 2004.

[209] I. N. Dimou, G. C. Manikis, and M. E. Zervakis, "Classifier fusion approaches for diagnostic cancer models," in *Proc. 28th Annu. Int. Conf. Eng. Med. Biol. Soc. (EMBS)*, 2006, pp. 5334–5337.

[210] N. Zhang, Q. Liao, S. Ruan, S. Lebonvallet, and Y. Zhu, "Multi-kernel SVM based classification for tumor segmentation by fusion of MRI images," in *Proc. IEEE Int. Workshop Imag. Syst. Techn. (IST)*, May 2009, pp. 71–75.

[211] Y. Huang, J. Zhang, Y. Zhao, and D. Ma, "Medical image retrieval with query-dependent feature fusion based on one-class SVM," in *Proc. IEEE 13th Int. Conf. Comput. Sci. Eng. (CSE)*, Dec. 2010, pp. 176–183.

[212] K. G. Nikolakopoulos, "Comparison of nine fusion techniques for very high resolution data," *Photogram. Eng. Remote Sens.*, vol. 74, no. 5, pp. 647–659, 2008.

[213] Q. Wei, N. Dobigeon, and J.-Y. Tourneret, "Fast fusion of multi-band images based on solving a Sylvester equation," *IEEE Trans. Image Process.*, vol. 24, no. 11, pp. 4109–4121, Nov. 2015.

[214] Q. Wei, N. Dobigeon, and J. Y. Tourneret, "Bayesian fusion of multi-band images," *IEEE J. Sel. Topics Signal Process.*, vol. 9, no. 6, pp. 1117–1127, Sep. 2015.

[215] M. Golipour, H. Ghassemian, and F. Mirzapour, "Integrating hierarchical segmentation maps with MRF prior for classification of hyperspectral images in a Bayesian framework," *IEEE Trans. Geosci. Remote Sens.*, vol. 54, no. 2, pp. 805–816, Feb. 2016.

[216] M. Xu, H. Chen, and P. K. Varshney, "An image fusion approach based on Markov random fields," *IEEE Trans. Geosci. Remote Sens.*, vol. 49, no. 12, pp. 5116–5127, Dec. 2011.

[217] R. S. Blum, "On multisensor image fusion performance limits from an estimation theory perspective," *Inf. Fusion*, vol. 7, no. 3, pp. 250–263, 2006.

[218] F. Tupin and M. Roux, "Markov random field on region adjacency graph for the fusion of SAR and optical data in radargrammetric applications," *IEEE Trans. Geosci. Remote Sens.*, vol. 43, no. 8, pp. 1920–1928, Aug. 2005.

[219] A. Dogra and P. Bhalla, "Image sharpening by Gaussian and butterworth high pass filter," *Biomed. Pharmacol. J.*, vol. 7, no. 2, pp. 707–713, 2014.

[220] A. Dogra and P. Bhalla, "CT and MRI brain images matching using ridgeness correlation," *Biomed. Pharmacol. J.*, vol. 7, no. 2, pp. 691–696, 2014.

[221] B. Goyal, S. Agrawal, B. S. Sohi, and A. Dogra, "Noise Reduction in MR brain image via various transform domain schemes," *Res. J. Pharmacy Technol.*, vol. 9, no. 7, pp. 919–924, 2016.

[222] B. Goyal, A. Dogra, S. Agrawal, and B. S. Sohi, "Dual Way Residue Noise Thresholding along with feature preservation," *Pattern Recognit. Lett.*, vol. 94, pp. 194–201, Jul. 2017.

[223] A. Dogra, "Performance comparison of different wavelet families based on bone vessel fusion," *Asian J. Pharmaceutics*, vol. 10, no. 4, 2017, pp. S791–S795.

[224] A. Arora *et al.*, "Development, characterization & processing of quantum dots for imaging in UV-visible range," *Int. J. Pharmacy Technol.*, vol. 8, no. 2, pp. 12811–12825, Jun. 2016.

[225] P. Shah, S. N. Merchant, and U. B. Desai, "Fusion of surveillance images in infrared and visible band using curvelet, wavelet and wavelet packet transform," *Int. J. Wavelets, Multiresolution Inf. Process.*, vol. 8, no. 2, pp. 271–292, 2010.

[226] P. Shah, S. N. Merchant, and U. B. Desai, "An efficient adaptive fusion scheme for multifocus images in wavelet domain using statistical properties of neighborhood," in *Proc. 14th Int. Conf. Inf. Fusion (FUSION)*, 2011, pp. 1–7.

[227] B. K. S. Kumar, "Multifocus and multispectral image fusion based on pixel significance using discrete cosine harmonic wavelet transform," *Signal, Image Video Process.*, vol. 7, no. 6, pp. 1125–1143, 2013.

[228] V. Petrovic and C. Xydeas, "Objective image fusion performance characterisation," in *Proc. 10th IEEE Int. Conf. Comput. Vis. (ICCV)*, vol. 2. Oct. 2005, pp. 1866–1871.

[229] J. Tian, L. Chen, L. Ma, and W. Yu, "Multi-focus image fusion using a bilateral gradient-based sharpness criterion," *Opt. Commun.*, vol. 284, no. 1, pp. 80–87, 2011.

[230] S. Li, X. Kang, J. Hu, and B. Yang, "Image matting for fusion of multi-focus images in dynamic scenes," *Inf. Fusion*, vol. 14, no. 2, pp. 147–162, 2013.

[231] S. Koduri, "Multisensor data fusion with singular value decomposition," in *Proc. 14th Int. Conf. Comput. Modelling Simulation (UKSim)*, 2012, pp. 422–426.

[232] J. Tian and L. Chen, "Adaptive multi-focus image fusion using a wavelet-based statistical sharpness measure," *Signal Process.*, vol. 92, no. 9, pp. 2137–2146, 2012.

[233] B. Jin, Z. Jing, and H. Pan, "Multi-modality image fusion via generalized riesz-wavelet transformation," *Trans. Internet Inf. Syst.*, vol. 8, no. 11, pp. 4118–4136, 2014.

[234] X. Kang, S. Li, and J. A. Benediktsson, "Feature extraction of hyperspectral images with image fusion and recursive filtering," *IEEE Trans. Geosci. Remote Sens.*, vol. 52, no. 6, pp. 3742–3752, Jun. 2014.

[235] Y. Liu, S. Liu, and Z. Wang, "Multi-focus image fusion with dense SIFT," *Inf. Fusion*, vol. 23, pp. 139–155, May 2015.

[236] Y. Liu and Z. Wang, "Dense SIFT for ghost-free multi-exposure fusion," *J. Vis. Commun. Image Represent.*, vol. 31, pp. 208–224, Aug. 2015.

[237] Y. Liu, X. Chen, R. K. Ward, and Z. J. Wang, "Image fusion with convolutional sparse representation," *IEEE Signal Process. Lett.*, vol. 23, no. 12, pp. 1882–1886, Dec. 2016.

[238] Y. Liu, X. Chen, H. Peng, and Z. Wang, "Multi-focus image fusion with a deep convolutional neural network," *Inf. Fusion*, vol. 36, pp. 191–207, Jul. 2017.

[239] J. Yang, Y. Li, J.C.-W. Chan, and Q. Shen, "Image fusion for spatial enhancement of hyperspectral image via pixel group based non-local sparse representation," *Remote Sens.*, vol. 9, no. 1, p. 53, 2017.

[240] Y. Fei, G. Wei, and S. Zongxi, "Medical image fusion based on feature extraction and sparse representation," *Int. J. Biomed. Imag.*, vol. 2017, Feb. 2017, Art. no. 3020461.

[241] S. G. Simone, A. Farina, F. C. Morabito, S. B. Serpico, and L. Bruzzone, "Image fusion techniques for remote sensing applications," *Inf. Fusion*, vol. 3, no. 1, pp. 3–15, 2002.

[242] T. Mertens, J. Kautz, and F. Van Reeth, "Exposure fusion: A simple and practical alternative to high dynamic range photography," *Comput. Graph. Forum*, vol. 28, no. 1, pp. 161–171, 2009.

[243] N. Al-Azzawi, W. Ahmed, and K. W. Abdullah, *Medical Image Fusion Schemes Using Contourlet Transform and PCA Bases*. Vukovar, Croatia: InTech, 2011.

[244] E. Daniel, J. Anitha, K. K. Kamaleshwaran, and I. Rani, "Optimum spectrum mask based medical image fusion using Gray Wolf Optimization," *Biomed. Signal Process. Control*, vol. 34, pp. 36–43, Apr. 2017.

[245] R. Van de Plas, J. Yang, J. Spraggins, and R. M. Caprioli, "Image fusion of mass spectrometry and microscopy: A multimodality paradigm for molecular tissue mapping," *Nature Methods*, vol. 12, no. 4, pp. 366–372, 2015.

[246] V. P. S. Naidu, "Discrete cosine transform-based image fusion," *Defence Sci. J.*, vol. 60, no. 1, p. 48, 2010.

[247] Y. Yang, W. Wan, S. Huang, F. Yuan, S. Yang, and Y. Que, "Remote sensing image fusion based on adaptive IHS and multiscale guided filter," *IEEE Access*, vol. 4, pp. 4573–4582, 2016.
[248] R. Restaino, G. Vivone, M. D. Mura, and J. Chanussot, "Fusion of multispectral and panchromatic images based on morphological operators," *IEEE Trans. Image Process.*, vol. 25, no. 6, pp. 2882–2895, Jun. 2016.
[249] X. Bai, M. Liu, Z. Chen, P. Wang, and Y. Zhang, "Multi-focus image fusion through gradient-based decision map construction and mathematical morphology," *IEEE Access*, vol. 4, pp. 4749–4760, 2016.
[250] B. Kang, W.-P. Zhu, and J. Yan, "Fusion framework for multi-focus images based on compressed sensing," *IET Image Process.*, vol. 7, no. 4, pp. 290–299, Jun. 2013.
[251] F. A. Al-Wassai, N. V. Kalyankar, and A. A. Al-Zaky. (Aug. 2011). "Multisensor images fusion based on feature-level." [Online]. Available: https://arxiv.org/abs/1108.4098
[252] S. S. Malik, B. J. Shivprasad, G. B. Maruthi, J. Kuriakose, and V. Amruth, "Feature level image fusion," in *Proc. Int. Conf., Emerg. Res. Comput., Inf., Commun. Appl. (ERCICA)*, Aug. 2013, pp. 566–574.
[253] A. J. Rashidi and M. H. Ghassemian, "A new approach for multi-system/sensor decision fusion based on joint measures," *Int. J. Inf. Acquisition*, vol. 1, no. 2, pp. 109–120, 2004.
[254] F. T. Mahmoudi, F. Samadzadegan, and P. Reinartz, "Object recognition based on the context aware decision-level fusion in multiviews imagery," *IEEE J. Sel. Topics Appl. Earth Observ. Remote Sens.*, vol. 8, no. 1, pp. 12–22, Jan. 2015.
[255] V. R. Pandit and R. J. Bhiwani, "Image fusion in remote sensing applications: A review," *Int. J. Comput. Appl.*, vol. 120, no. 10, pp. 22–32, Jun. 2015.
[256] K. Ma, H. Li, H. Yong, Z. Wang, D. Meng, and L. Zhang, "Robust multi-exposure image fusion: A structural patch decomposition approach," *IEEE Trans. Image Process.*, vol. 26, no. 5, pp. 2519–2532, May 2017.
[257] N. E. Huang *et al.*, "The empirical mode decomposition and the Hilbert spectrum for nonlinear and non-stationary time series analysis," *Proc. Roy. Soc. London Ser. A, Math., Phys. Eng. Sci.*, vol. 454, no. 1971, pp. 903–995, Mar. 1998.
[258] T.-A. Teo and C.-C. Lau, "Pyramid-based image empirical mode decomposition for the fusion of multispectral and panchromatic images," *EURASIP J. Adv. Signal Process.*, vol. 2012, no. 1, p. 4, 2012.
[259] S. M. U. Abdullah, N. U. Rehman, M. M. Khan, and D. P. Mandic, "A multivariate empirical mode decomposition based approach to pansharpening," *IEEE Trans. Geosci. Remote Sens.*, vol. 53, no. 7, pp. 3974–3984, Jul. 2015.
[260] N. Rehman, S. Ehsan, S. M. U. Abdullah, M. J. Akhtar, D. P. Mandic, and K. D. McDonald-Maier, "Multi-scale pixel-based image fusion using multivariate empirical mode decomposition," *Sensors*, vol. 15, no. 5, pp. 10923–10947, 2015.
[261] A. Toet, "Image fusion by a ratio of low-pass pyramid," *Pattern Recognit. Lett.*, vol. 9, no. 4, pp. 245–253, 1989.
[262] P. M. Zeeuw, *Wavelet and Image Fusion*. Amsterdam, The Netherlands: CWI, Mar. 1998. [Online]. Available: http://www.cwi.nl/~pauldz/
[263] V. P. S. Naidu, "Image fusion technique using multi-resolution singular value decomposition," *Defence Sci. J.*, vol. 61, no. 5, p. 479, 2011.
[264] J. Ma, C. Chen, C. Li, and J. Huang, "Infrared and visible image fusion via gradient transfer and total variation minimization," *Inf. Fusion*, vol. 31, pp. 100–109, Sep. 2016.
[265] *Basic of Image Fusion*. Accessed on Apr. 2017. [Online]. Available: https://www.pantechsolutions.net/image-processing-projects/
[266] H. Li, L. Li, and J. Zhang, "Multi-focus image fusion based on sparse feature matrix decomposition and morphological filtering," *Opt. Commun.*, vol. 342, pp. 1–11, May 2015.
[267] Q. Zhang, Y. Liu, R. S. Blum, J. Han, and D. Tao. (Feb. 2017). "Sparse representation based multi-sensor image fusion: A review." [Online]. Available: https://arxiv.org/abs/1702.03515
[268] B. Miles, I. B. Ayed, M. W. K. Law, G. Garvin, A. Fenster, and S. Li, "Spine image fusion via graph cuts," *IEEE Trans. Biomed. Eng.*, vol. 60, no. 7, pp. 1841–1850, Jul. 2013.
[269] R. Shen, I. Cheng, J. Shi, and A. Basu, "Generalized random walks for fusion of multi-exposure images," *IEEE Trans. Image Process.*, vol. 20, no. 12, pp. 3634–3646, Dec. 2011.
[270] K.-L. Hua, H.-C. Wang, A. H. Rusdi, and S.-Y. Jiang, "A novel multi-focus image fusion algorithm based on random walks," *J. Vis. Commun. Image Represent.*, vol. 25, no. 5, pp. 951–962, 2014.

AYUSH DOGRA received the B.Tech. degree from Guru Nanak Dev University, the M.Tech. degree from Punjabi university, Patiala, and the M.B.A. degree from IGNOU, New Delhi. He is currently pursuing the Ph.D. degree with Panjab University, Chandigarh. He has 15 papers to his credit, which consists of SCOPUS and SCIE indexed papers. His research interests are image registration, image fusion, image enhancement, and image denoising.

BHAWNA GOYAL received the B.E. degree in electronics and communication engineering from GNDU, Amritsar, India, in 2012, and the M.Tech. degree in ECE from the PEC University of technology, Chandigarh, in 2014. She is currently pursuing the Ph.D. degree with Panjab University, Chandigarh. She has five publications to her account out of which two are SCI indexed articles are rest of them are SCOPUS indexed. Her research interests are image denoising, image enhancement, image fusion, and optical communication.

SUNIL AGRAWAL received the master's degree in engineering from Thapar University, Patiala, and the Ph.D. degree from Panjab University (PU), Chandigarh. He is currently a Professor with UIET, PU. He has many publications to his account out of which many are SCIE and SCOPUS indexed articles. His main areas research is wireless communication, artificial intelligence, image processing, and optical communication.